

Estuaries and Coasts

Salt marsh accretion and storm tide variation: An example from a barrier island in the North Sea

--Manuscript Draft--

Manuscript Number:	ESCO-D-11-00016R2
Full Title:	Salt marsh accretion and storm tide variation: An example from a barrier island in the North Sea
Article Type:	Original Report
Keywords:	Salt marsh, accretion rate, geochronology, storm activity, barrier island, Sylt
Corresponding Author:	Mark Schürch, Diploma University of Kiel / Institute of Geography Kiel, GERMANY
Corresponding Author Secondary Information:	
Corresponding Author's Institution:	University of Kiel / Institute of Geography
Corresponding Author's Secondary Institution:	
First Author:	Mark Schürch, Diploma
First Author Secondary Information:	
All Authors:	Mark Schürch, Diploma
	John Rapaglia, PhD
	Volker Liebetrau, PhD
	Athanasios Vafeidis, Junior Professor
	Karsten Reise, Professor
All Authors Secondary Information:	
Abstract:	We reconstruct past accretion rates of a salt marsh on the island of Sylt, Germany, using measurements of the radioisotopes ²¹⁰ Pb and ¹³⁷ Cs, as well as historical aerial photographs. Results from three cores indicate accretion rates varying between 1 and 16 mm yr ⁻¹ . Comparisons with tide gauge data show that high accretion rates during the 1980's and 1990's coincide with periods of increased storm activity. We identify a critical inundation height of 18 cm below which the strength of a storm seems to positively influence salt marsh accretion rates, and above which the frequency of storms becomes the major factor. Beyond the impact of sea level rise, we conclude that for high inundation heights occurring in lower marsh zones, the mean strength of storms is predominantly affecting marsh accretion, while for low inundation heights, occurring in higher marsh zones, the frequency of storms is the dominant driver for marsh accretion.

COVER LETTER - SUBMISSION OF REVISED MANUSCRIPT

Kiel, October 27, 2011

Subject: **SUBMISSION OF REVISED MANUSCRIPT:**

“Salt marsh accretion and storm tide variation: An example from a barrier island in the North Sea”

Dear Editor(s),

I would like to thank you for the evaluation of the revised manuscript (first submitted on the 11th of January 2011). We have addressed all the minor modifications suggested by the 2 reviewers and have revised the manuscript accordingly.

Based on the suggestions of reviewer #1, we revised figure 1 and all other figures by increasing their resolution and incorporating the other suggested modifications. Furthermore, we converted the bulk density numbers to SI-units and double-checked all the numbers throughout the manuscript. We are confident that all numbers are now correct.

Addressing the comments of reviewer #2, we rewrote the abstract, including the methods of how we constructed the presented geochronology and focusing on historical responses of salt marsh accretion rates in relation to storm pattern rather than future predictions. We also made some corrections within the manuscript removing speculative parts about future developments. Concerning the estimation of autocompaction, we included a rationale for only using the upper 5 cm of the cores for analysis within the “Methods” section.

The additional modifications suggested by the reviewers have further improved the manuscript and we are confident that the paper is now ready for publication.

Please find enclosed the revised manuscript, together with the detailed answers to the comments of the 2 reviewers.

Sincerely yours

Mark Schürch

Reply to reviewer #1

Please note: Replies in violet are the most recent replies to the 2nd review of reviewer #1.

Comments from review #1

Study site

Line 81. Are these coordinates right? As far as I can tell from Google Earth, this is a site in west Jutland in Denmark??

Coordinates were corrected to 54°54'N, 008°20'E.

Please state the coordinates for sampling site. You need to be more precise. Now we are on Sild, but in the middle of a town. Include the seconds as well.

Coordinates were changed to 54°47'18''N / 008°17'30''E. This corresponds to a location in the middle of the investigated salt marsh.

Figure 1. This is a poor figure. The top figure seems to be out of proportions.

The coordinate system of the top figure was changed from WGS 1984 to ETRS 1989 UTM, this will hopefully help the reader understand the figure.

This is still a poor figure. The resolution seems to be too low (at least in my copy). In the bottom right figure I can't find neither the Path/Road nor the Veg. not specified. Either delete these two legends or find a way to make them clear on the figure.

We increased the resolution of figure 1 and all other figures to 300 dpi. We deleted the "Road / Path" entry from the legend and made the "Vegetation not specified" more visible in the figure.

New comments for review #2

S 12 RESULTS

Please use SI units and state the dry bulk density in kg m⁻³

We changed the units of bulk density from kg dm⁻³ to kg m⁻³. We also changed the respective numbers in figure 3.

S 12 line 289. I think there is a typo here, the dry bulk density cannot be 9.39 kg dm⁻³ (pure solid quartz is around 2.6 kg dm⁻³).

The value was corrected to 939 kg m⁻³.

S 12 Line 299. The same, the DBD is too high at 5-6 kg dm⁻³

The values were corrected to 500-600 kg m⁻³.

S 12 line 293. The same (3.25 & 6.56 kg dm⁻³)

The values were corrected to 325 and 656 kg m⁻³.

S 13 line 294. The same (4.5-5 kg dm⁻³)

The values were corrected to 450-500 kg m⁻³.

S 13 line 304-308. I think you mean decrease instead of increase in the upper 5 cm. Is the decrease significant?

Since all other bulk density values are reported from a top-down perspective, we would rather use the same method here. This means that it is an increase with depth.

The increase can be represented by a logarithmic regression at a significance level of $p < 0.02$. The paragraph was reworded respectively: *“The increase of bulk density within the uppermost 5 cm of core S1 was found to fit the logarithmic model (equation 6; $R^2 = 0.97$, $p < 0.02$), which is considered as evidence for autocompaction. Model parameters A and B were estimated to be 0.0879 and 0.3791, respectively. The autocompaction rate during the growth of the salt marsh therefore averages 1 mm yr⁻¹.”*

As far as I can tell from fig 3, all densities are below 2 kg dm⁻³, and most of the fine grained material is around 0.5 kg dm⁻³.

In fact, most fine grained material is around 500 kg m⁻³ in cores S2 and S3. However this is different in S1, where bulk density increases with depth from about 325 to 656 kg m⁻³. This should also be detectable in figure 3.

S 16 line 370. The acc rate of 1.5 – 1.8 mm / yr does not correspond with the numbers in Table 1 (1 – 1.2 mm/yr)

The numbers in the text were changed to 1-1.2 kg m⁻³.

IN GENERAL, THE AUTHORS SHOULD DOBBLE CHECK ALL NUMBERS IN THE MANUSCRIPT.

All numbers were double checked: Besides a few minor changes, we have corrected the value for the mean accretion rate in S3 from 4 mm yr⁻¹ to 2.5 mm yr⁻¹ and the threshold for the inundation depth from 26 cm to 18 cm.

We are sure that ALL number are correct now.

S 19 line 444. Don't you mean S1 and S2. As far as I can tell S3 does not contain Cs137.

We do mean core S2 and S3. The fact that S3 does not show a ¹³⁷Cs peak supports the dating since this suggests that the marsh started to develop after 1986. A respective explanation was added: *“The absence of a peak in core S3 also supports what we can observe in the aerial photographs, as well as the ²¹⁰Pb dating suggesting that the marsh development started after 1988.”*

Figures: you seem to have exchanged fig 5 and fig 6.

Revised as suggested.

Fig 12: you need a label on the x-axis

We added the following label for the x-axis: *“Storm water level (m above NN)”*.

Replies to reviewer #2

Reviewer #2: I have read the article by Schuerch et al., in which they use sedimentary geochronologies to examine how marshes in the Wadden Sea have responded to climate variability over the past century, and how they might respond to future changes in climate over the next century. Overall, this is a pretty good paper. However, I think it needs one substantial change and several more minor ones before it can be accepted for final publication.

Thank you for reviewing the paper and for your very valuable feedback. We revised our paper according to your suggestions and are happy to see that the paper has considerably gained from these changes.

Major changes:

The most important changes that are needed are with respect to the authors' analysis of how these marshes will respond to future changes in climate. In their abstract, they write, "Future development of low-lying marsh zones will therefore be controlled by mean high water levels, while upper marsh accretion rates will be controlled by storm activity. We suggest that climate change has a higher impact on the marsh zonation rather than on marsh survival." This statement is too broad.

This sentence was worded: *"Beyond the impact of sea level rise, we conclude that for high inundation heights occurring in lower marsh zones, the mean strength of storms is predominantly affecting marsh accretion, while for low inundation heights, occurring in higher marsh zones, the frequency of storms is the dominant driver for marsh accretion."*

In this paper the authors have mostly measured processes that occur along the vertical axis, and have not really considered what can happen along the horizontal plane. (Aside from a brief examination of aerial photographs). In other words, most of their data is core data, and not a detailed analysis of spatial change, such as might be done with a GIS. The authors don't seem to consider whether increased storm activity could increase shoreface erosion, and how a decreasing marsh width might impact interior regions of the marsh. This problem needs to be corrected.

We are aware of the fact that less consideration has been given to lateral marsh development within our study. In order to emphasize this limitation we added the following phrases at the beginning of the "Influence of storm on accretion" ("Discussion"): *"The analysis presented in this study focuses on the historical vertical development of a single salt marsh. It is shown that an increase in storminess positively correlates with marsh accretion rates. While many authors have focused on the destructive, erosional influence of storms on salt marshes (e.g. Callaghan et al. 2010, Mariotti and Fagherazzi 2010, van de Koppel et al. 2005), our methods are not able to reproduce the lateral marsh development and their implications on accretion processes, but rather the vertical marsh accretion."*

I would suggest that the authors

1) focus more on their analysis of the past response of marshes to storms and sea level change, which is very well done, rather than speculate on future changes, which is more tenuous.

We removed the paragraph "Future marsh development". As you mention, it is indeed not sufficiently supported by the available data. Consequently we also reworded the respective paragraph in the "Conclusions" focusing more on what we could observe rather than what we expect for the future.

2) recognize the difference between things that are measured in a core and things that occur in the lateral environment.

The concept of the critical inundation height found in our data has spatial implications, since inundation depth is higher in the low marsh zone than in the high marsh zone. We reworded the respective phrase in the abstract (as described above) to make clear that this is the only spatial implication that we are suggesting.

Minor changes:

Abstract: The abstract needs a bit of rewording. The authors should avoid the passive voice whenever possible. Also, the authors could include a few more specifics- such as by noting how the geochronologies were constructed.

The abstract was reworded. We replaced the formulations with passive voice and added the three methods employed for the reconstruction of historic marsh accretion.

Lines 35-36. The Kirwan citations are not right citations. It would be better to cite Redfield (1972) or Orson (1985).

Revised as suggested.

Line 54. The authors have a comma after the K+G paper, but I think they mean to have a period.

The comma follows the introductory clause "While ..." and separates it from the main clause. We think that the comma is grammatically correct.

Line 79 - an elsewhere. The authors refer to figures using lowercase letters. I would prefer to see the word figure capitalized and abbreviated- as "Fig. 1." However, I will defer to the editorial staff for on any final determination of the article's style.

Revised as suggested.

Line 126. The authors should prove, or provide data, indicating that compaction was negligible.

The following sentence, summarizing the data that underlies this statement is added: *"Compaction during core collection was measured in situ as the difference between the measures from the top of the PVC-tube to the salt marsh surface outside and inside the core. This difference was found vary between 2 and 4 % of the core length (in all three cores) and was therefore assumed to be negligible."*

Lines 170-172. Why was autocompaction only investigated in the top 5 cm. Certainly it can happen anywhere in the core. This seems weird and either needs to be explained in more detail or the analysis should be conducted on the entire core. Even if Bartholdy (2010) present a method to use this, the rationale for using their method must be explained in sufficient detail in the paper for that rationale to stand alone.

We added an explanation why we employed the method following the mentioned sentence: *"[...], since variability of bulk density triggered by changes of grain size and organic carbon content in the lower parts of the core was too large to derive reliable estimates for autocompaction."*

Line 214. De Groot is not the right citation. This was understood long before 2009. You might try Compton (1923) instead.

Revised as suggested.

Line 280. I believe this sentence should read, "Fine grained sediments are?."

Revised as suggested.

Line 284- 308. The authors need to be more careful about the number of significant figures attached to the bulk density values. Are 4 significant figures really appropriate.

All bulk density estimates were rounded to no decimal figures (applying the SI unit kg m^{-3}).

Also, I am not used to seeing bulk densities listed as kg/dm^3 , and instead would prefer to see them as g/cm^3 or kg/m^3 unless the authors have a compelling reason to do otherwise.

The unit of bulk density was changed to kg/m^3 .

Line 326 (and elsewhere). For excess ^{210}Pb I am used to seeing the subscript XS rather than exc, and I would prefer to see that used - unless the authors have a compelling reason to do otherwise.

Revised as suggested.

Line 516. General comment: I very much like the authors analysis of storm influence on marsh accretion. It would be interesting to hear some discussion as to whether the authors think this is due to the positive shift in the NAO as some (e.g. Hurrell et al., 2001) or whether this is an imprint of an acceleration in global sea level rise rates as others (e.g. Kolker et al., 2010), have noted.

We are aware of the close relationship between storminess and the NAO index suggested by some authors, but we could not find this relationship in our data. We think that a positive shift in the NAO index could positively influence salt marsh accretion. However our data does not prove this hypothesis sufficiently to discuss it within the paper. We currently conduct further investigations on separating the different climatic influences on salt marsh accretion by means of modeling.

Line 588. The authors write, " No confident predictions for the future development of storm patterns are available at the moment." This sentence is a bit poorly constructed and should be rewritten.

As stated earlier this paragraph was removed altogether.

Figure 8. The horizontal lines in this figure are kind of ugly. I think that this happens when you make figures in MS excel. There is a way to get rid of these lines, and this should be done.

Revised as suggested (all figures were compiled in Matlab).

1 Salt marsh accretion and storm tide variation: 2 An example from a barrier island in the North 3 Sea

4 M. Schuerch¹, J. Rapaglia¹, V. Liebetrau², A. Vafeidis¹, K. Reise³

5 ¹*University of Kiel, Institute of Geography, “The Future Ocean” Excellence*
6 *Cluster, Germany*

7 ²*Leibniz Institute of Marine Science, IFM-GEOMAR, “The Future Ocean”*
8 *Excellence Cluster, Kiel, Germany*

9 ³*Alfred Wegner Institute for Polar and Marine Research, Waddenseastation Sylt,*
10 *Germany*

11 Corresponding address: Mark Schürch, schuerch@geographie.uni-kiel.de, +49 431 8805641
12 (phone), +49 431 8804658 (fax)

13

14 ABSTRACT

15 We reconstruct past accretion rates of a salt marsh on the island of Sylt, Germany, using
16 measurements of the radioisotopes ²¹⁰Pb and ¹³⁷Cs, as well as historical aerial photographs.
17 Results from three cores indicate accretion rates varying between 1 and 16 mm yr⁻¹. Comparisons
18 with tide gauge data show that high accretion rates during the 1980's and 1990's coincide with
19 periods of increased storm activity. We identify a critical inundation height of 18 cm below which
20 the strength of a storm seems to positively influence salt marsh accretion rates, and above which
21 the frequency of storms becomes the major factor. Beyond the impact of sea level rise, we
22 conclude that for high inundation heights occurring in lower marsh zones, the mean strength of
23 storms is predominantly affecting marsh accretion, while for low inundation heights, occurring in
24 higher marsh zones, the frequency of storms is the dominant driver for marsh accretion.

25 .

26 KEYWORDS

27 *Salt marsh, accretion rate, geochronology, storm activity, barrier island, Sylt*

28 INTRODUCTION

29 Coastal salt marshes in the Wadden Sea (southeastern North Sea) are abundant
30 leeward of the East Frisian and North Frisian barrier islands as well as in front of
31 the dike system on the Dutch-German-Danish North Sea coast. Salt marshes serve
32 as coastal protection structures by reducing the impact of waves on the upper
33 shoreline (e.g. Möller, 2006) and as important habitats for specialized plants and
34 animals including migratory and breeding waterfowl, and breeding birds (Reise et
35 al., 2010). The existence of salt marshes is critically dependent on how fast
36 sediment accretes relative to sea level rise (Orson et al., 1985; Redfield, 1972).
37 Salt marshes are complex coastal features, governed by various physical and
38 biological processes creating a system that exists in dynamic equilibrium with
39 relative sea level rise (RSLR; Allen, 2000). Salt marsh accretion, defined as the
40 vertical growth of the marsh, occurs when organic and/or inorganic sediments are
41 deposited onto the marsh during inundation (allochthonous growth), as well as
42 when salt marsh plants grow and decompose (autochthonous growth; Dijkema,
43 1987; Kolker et al., 2009). Projected acceleration in SLR, however, may outpace
44 accretion rates in the future, if an insufficient amount of material is deposited on
45 the marsh surface (Kirwan and Temmerman, 2009; Orson et al., 1985). Several
46 investigators studied marsh response to mean sea level rise (French, 1993; Kirwan
47 and Temmerman, 2009; e.g. Orson et al., 1985; Reed, 1995), others investigated
48 the influence of tidal range on salt marsh accretion (e.g. Chmura et al., 2001;
49 Harrison and Bloom, 1977; Kirwan and Guntenspergen, 2010), but relatively little
50 literature is available discussing the impact of non-tidal short-term sea level
51 variations on salt marsh accretion (Bartholdy et al., 2004; French, 2006; Kolker et
52 al., 2009; Temmerman et al., 2003b). While it is a widespread assumption that

53 macrotidal environments are more resilient against SLR than microtidal
54 environments (Kirwan and Guntenspergen, 2010), Allen (2000) and Kolker et al.
55 (2009) conclude that marsh accretion is dominated by wind-induced (short-term)
56 sea level variations in microtidal, and by SLR-induced long-term sea level
57 variations in macrotidal environments. It remains unclear how wind-induced sea
58 level variations enhance the resilience of the salt marsh, and in particular, whether
59 many minor storms are more effective in triggering accretion than a few major
60 storms. This is noteworthy as certain studies suggest that the storm activity in the
61 German Bight has increased in recent years and will most likely increase in the
62 near future leading to more frequent storm surges and/or higher storm surge water
63 levels (Beniston et al., 2007; Fischer-Bruns et al., 2005; Rockel and Woth, 2007;
64 von Storch and Weisse, 2008; Woth et al., 2006).

65 The goal of this work is to reconstruct the development of a back-barrier salt
66 marsh on the island of Sylt, Germany, by using both ^{210}Pb and ^{137}Cs as
67 geochronometers. ^{210}Pb and ^{137}Cs are often used for studying soil and sediment
68 processes (Armentano and Woodwell, 1975; Delaune et al., 1978; Goodbred and
69 Kuehl, 1998; He and Walling, 1996b; Kolker et al., 2009). These data will be
70 combined with information gathered from aerial photographs. We report how the
71 marsh has been growing during the last decades and compare accretion rates with
72 historical tide gauge data in order to infer how storm activity affects marsh
73 accretion and its resilience against accelerated SLR.

74 **Study site**

75 The island of Sylt is located in the German Wadden Sea ($54^{\circ}47'18''\text{N}$,
76 $008^{\circ}17'30''\text{E}$), in the south-eastern North Sea (Fig. 1). Its core is made of
77 Pleistocene protruding outcrops. About 7000 years B.P., during a period of SLR

78 deceleration (Milne et al., 2005), local sea level reached its current position and
79 sandy spits were formed north and south of the original Pleistocene outcrop
80 (Ahrendt and Thiede, 2001). Sylt is an elongated barrier island with a total area of
81 99 km² extending 40 km from north to south and ranging from 1 to 13 km in
82 width (Kelletat, 1992). The western coastline is characterized by extensive
83 beaches and dunes, and, due to a relatively steep offshore elevation gradient, it is
84 exposed to highly energetic wave activity from the North Sea (Ahrendt and
85 Köster, 1998). The sheltered eastern coastline is fringed by extensive tidal flats.
86 Salt marshes are found in the transition zone from dunes to tidal flats and have a
87 total area of approximately 5 km² (TMAP - The Trilateral Monitoring and
88 Assessment Program 2006).

89 The mean tidal range, as of 2010, at the nearby tide gauge *Hörnum Hafen* is
90 2.06 m (WSA - Wasser- und Schifffahrtsamt Tönning, 2007), varying from 1.8 m
91 at neap tide to 2.3 m at spring tide (BSH - Bundesamt für Seeschifffahrt und
92 Hydrographie, 2008). Tidal range has constantly increased in the Wadden Sea,
93 including the *Hörnumtief*, since 1955 (Jensen and Mudersbach, 2004).

94 The immediate study area is located in the southern third of Sylt between the
95 villages of Rantum and Hörnum, and is characterized by the typical morphology
96 of a barrier island. A transect from the open North Sea to the tidal flats is marked
97 by a sequence of beaches, dunes, and salt marshes (Hildebrandt et al., 1993).

98 These dunes developed a dense grass and scrub vegetation and became stable, as a
99 consequence of intense planting activities since 1864 (ALW - Amt für Land- und
100 Wasserwirtschaft Husum, 1997). The area of the investigated marsh is about
101 0.3 km², with a length of about 2 km and a width ranging from 80 m to 280 m.
102 The salt marsh itself has a typical zonation ranging from pioneer marsh vegetation
103 at the seaward edge to high marsh vegetation close to the foot of the dunes (Fig.

104 1). The pioneer marsh is dominated by the introduced cordgrass *Spartina anglica*,
105 the low marsh zone is dominated by *Atriplex portulacoides*, and the high marsh
106 zone by *Juncus gerardi* and *Elymus athericus*. The vegetation is not grazed by
107 domestic livestock.

108 The elevation of the salt marsh ranges from about 0.7 to 1.5 m above NN (NN:
109 German reference datum; Fig. 2), while the mean high water level (MHW) is at
110 about 1 m (NN; WSA - Wasser- und Schiffahrtsamt Tönning, 2007). The
111 topography of the marsh is rather homogeneous, with a small marsh cliff (10-
112 20 cm height) at the transition from pioneer to low marsh (Fig. 2). It is therefore
113 assumed possible to reconstruct the historic evolution of this salt marsh by
114 analyzing one transect only.

115 **METHODS AND ANALYSIS**

116 **Sample collection and preparation**

117 Three marsh cores were collected on 22 January 2009 using PVC tubes with an
118 inner diameter of 11.8 cm. Cores were collected on a shore-normal transect,
119 within the three dominant vegetation zones (Fig. 1, 2) and had a length of about
120 50-70 cm. S3, the most seaward core, was collected about 30 m from the seaward
121 edge of the pioneer marsh, while S2 and S1 were located about 60 m and 110 m
122 inland from the seaward edge respectively (Fig. 2). The large diameter of the tube
123 was chosen in order to reduce possible compaction of the soil during collection, as
124 well as to amass a large volume of material for accurate analysis. Compaction
125 during core collection was measured in situ as the difference between the
126 measures from the top of the PVC-tube to the salt marsh surface outside and

127 inside the core. This difference was found to vary between 2 and 4 % of the core
128 length (in all three cores) and was therefore assumed to be negligible.

129 The transect where the cores were taken was leveled by hand using a dumpy level
130 on a tripod. The height of the (seaward) starting point was determined by
131 comparison of measured flooding and HW times between the starting point and
132 the tide gauge in *Hörnum Hafen*. Elevations of the 3 core locations, as of today,
133 are 0.94 m (S3), 1.34 m (S2) and 1.44 m (S1) above NN (Fig. 2). S3 is the only
134 core location that is regularly inundated, while S1 and S2 are only inundated
135 during storm tides.

136 After extraction, the cores were sliced into layers with a thickness of 1-5 cm. The
137 thickness of the layers progressively increased towards the bottom of the core.

138 The sediment was freeze-dried and ground manually in order to disintegrate the
139 conglomerates of sediment. The ground material was filled into Petri dishes with a
140 diameter of 52 mm and embedded into epoxy resin, which prevented ^{222}Rn from
141 degassing. The dry weight of the aliquots embedded for radiometric analysis
142 ranged from 17.25 to 43.44 g. Samples were allowed to sit for at least 3 weeks in
143 order to reach equilibrium between ^{226}Ra and ^{214}Bi before analysis.

144 **Sedimentology: Grain size, organic carbon content, and bulk density**

145 Salt marsh sediment was analyzed for grain size, organic carbon content, and bulk
146 density in order to derive the depths of the base layer and for calculation of
147 radioisotope inventories. Grain size measurements were conducted using laser
148 diffractometry (Malvern Mastersizer 2000). Although this method is supposed to
149 measure grain sizes ranging from 0.02 to 2000 μm (Malvern Instruments Ltd,
150 2010), gradually increasing uncertainties in the coarser spectrum of grain sizes
151 were observed during pre-measurements. Therefore, the sediment was sieved at

152 1000 μm before the measurements. The preparation of the samples included the
 153 destruction of organic carbon, using H_2O_2 , and iron if necessary, using sodium
 154 bicarbonate, sodium citrate, and sodium dithionite. The measurements were
 155 conducted at obscuration rates between 5 and 30 %.

156 The organic carbon content was measured using the element analyzer Euro EA,
 157 which performs C/N analysis. The organic carbon is oxydized in the system and
 158 escapes as CO_2 into a gas chromatographer where total C (and N) content is
 159 determined.

160 The bulk density (ρ) was indirectly calculated from the organic carbon and the
 161 water content (O_C and W) in the samples as not enough sample material was
 162 available in the upper layers for direct measurement. Assuming a constant density
 163 for water ($\rho_w=1.02 \text{ g cm}^{-3}$) and for mineral and organic matter ($\rho_M=2.6 \text{ g cm}^{-3}$,
 164 $\rho_O=1.2 \text{ g cm}^{-3}$ respectively), the bulk density was calculated using the following
 165 formula (Kolker et al., 2009):

$$166 \quad \rho = \frac{1-W}{\frac{W}{\rho_w} + \frac{1-W}{(1-O_C * \rho_M) + (O_C * \rho_O)}} \quad (5)$$

167 Additional measurements on dry bulk density and relative water content were
 168 conducted on cores extracted on the 18 May 2011 in order to validate these bulk
 169 density calculations. It was shown that the results of the model fit the measured
 170 data ($R^2=0.98$, $p<0.01$).

171 **Assessment of autocompaction**

172 Bulk density calculations were used for the assessment of autocompaction within
 173 the cores S1, S2, and S3. Bulk densities within the uppermost 5 cm of the salt
 174 marsh cores were investigated for autocompaction (Bartholdy et al., 2010), since

175 variability of bulk density triggered by changes of grain size and organic carbon
 176 content in the lower parts of the core was too large to derive reliable estimates for
 177 autocompaction. A logarithmic curve (equation 6) was fitted through the
 178 calculated bulk density data (BDD) within the uppermost 5 cm.

$$179 \quad BDD = A * \ln(z) + B \quad (6)$$

180 where A and B are constants to be optimized and z is the depth of the respective
 181 salt marsh layer.

182 If the model was found to significantly represent the bulk density data ($p < 0.05$),
 183 autocompaction was included into the calculation of accretion rates by
 184 decompacting the core. Decompaction was performed by calculating the thickness
 185 of a layer in depth z (T_z) to the time when it was deposited using the inverse
 186 version of the equation presented by Williams et al. (2003):

$$187 \quad T_z = \frac{BDD_z}{BDD_0} * T_0 \quad (7)$$

188 where BDD_0 and T_0 are the bulk dry density and the thickness of today's surface
 189 layer, respectively.

190 **Radiometric measurements**

191 ^{137}Cs ($t_{1/2} = 30.2$ years) is a product of nuclear fission, and is highly particle
 192 reactive (He and Walling, 1996b). In Europe, it is marked by two main periods of
 193 atmospheric fallout (1963 and 1986) producing two useful marker horizons
 194 (Delaune et al., 1978; Kirchner and Ehlers, 1998; Pedersen et al., 2007). The ^{137}Cs
 195 peak around 1963 is produced by a series of tests of nuclear bombs during the
 196 1950's and 1960's, while the 1986-peak is a result of the nuclear disaster in
 197 Chernobyl. Some authors have found an additional ^{137}Cs signal in cores taken
 198 along the North and the Baltic Sea, peaking between 1974 and 1977 (Andersen et

199 al., 2000; Kunzendorf et al., 1998). However given the low initial activity and the
200 30 year half-life of ^{137}Cs , these activities are probably below detection limits
201 today. ^{210}Pb ($t_{1/2}=22.3$ years), on the other hand, is constantly being supplied from
202 the atmosphere via the decay of its grandparent nuclide ^{222}Rn (Koide et al., 1972;
203 Walling et al., 2003). This continuous deposition makes ^{210}Pb an excellent
204 geochronometer for deriving accretion rates in coastal salt marshes (Appleby and
205 Oldfield, 1978; Appleby and Oldfield, 1983; Bartholdy et al., 2004; Bellucci et
206 al., 2007; Kirchner and Ehlers, 1998).

207 A low-background coaxial Ge(Li)detector was employed to measure total gamma-
208 ray activity of ^{210}Pb , ^{226}Ra , and ^{137}Cs . It is a non-destructive counting method that
209 allows simultaneous measurement of all three radionuclides (Nikulina, 2008).

210 Measurement of ^{226}Ra is necessary, because it is a proxy for supported ^{210}Pb . The
211 analysis was conducted by the 'Laboratory for Radioisotopes' in Goettingen,
212 Germany. ^{210}Pb was measured via its gamma peak at 46.6 keV, ^{137}Cs via its peak
213 at 661.7 keV, and ^{226}Ra via the peaks of its granddaughters ^{214}Pb and ^{214}Bi at
214 352 keV and 609.3 keV/1120.3 keV respectively. The measurement time for all
215 samples was 250,000 seconds.

216 **Errors / Detection limit**

217 Errors generally increase towards the low energy gamma ray spectrum, since the
218 background radiation is elevated as a consequence of the Compton effect of
219 higher energetic radionuclides (Compton, 1923). Meanwhile for higher energy
220 spectra, the background radiation decreases continuously. For ^{210}Pb that is
221 measured at 46.6 keV (very low energy) this is of particular importance, since the
222 background radiation within the sample may be elevated above the ^{210}Pb activity
223 of the soil sample, resulting in measurements below detection limit.

224 Another source of error for radiometric measurements is the background radiation
225 of the environment, which is quantified by measuring a parallel blank sample and
226 minimized by increasing the sample volume as well as the counting time.
227 The combined “internal” and environmental background radiation at 46.6 keV is
228 therefore higher than the activity measured for ^{226}Ra in higher energy spectra and
229 detection limits can be included into the analysis as maximum values for ^{210}Pb
230 activities.

231 **Dating model**

232 The constant rate of supply model (CRS) is employed for the dating of sediment
233 characterized by variations of initial concentrations (Appleby and Oldfield, 1978;
234 Appleby and Oldfield, 1983). It is therefore useful in study sites with irregular
235 inundation, where accretion rates strongly vary with time. This model allows for
236 the calculation of the age of the sediment by using radioisotope inventories
237 (Appleby and Oldfield, 1978; Kolker et al., 2009).

238 Due to the relative elevation of the core locations within the tidal frame (Fig. 2),
239 irregular inundation occurs during storm surges, negating the assumption that
240 accretion rates are constant over time. Therefore the CRS model was used for this
241 study.

242 **Aerial photographs**

243 Aerial photographs of the investigated area, provided by the *Landesbetrieb für*
244 *Küstenschutz, Nationalpark und Meeresschutz Schleswig-Holstein (LKN-SH)*,
245 were utilized in order to analyze the historic extension of the salt marsh during the
246 last century and to verify the radiometric measurements. Photographs were
247 available from 1937, 1958, 1988, 1999, 2003, and 2007. After georeferencing the

248 pictures and overlaying the core locations, visual interpretation was performed in
249 order to classify the core location into the categories ‘marsh’ and ‘no marsh’.

250 **Hydrological data**

251 Annual data about mean sea level (MSL) were calculated from annual mean high
252 water (MHW) and mean low water (MLW) levels (Hofstede 2010: pers. comm.).

253 Storm frequency and storm intensity were aggregated from the high water levels,
254 collected for every tidal cycle between 1938 and 2007 (Wahl 2010: pers. comm.,
255 Wahl et al. 2011). Eustatic sea level rise was included into the analysis as an
256 underlying trend that was removed from the original dataset before storm
257 parameterization was conducted. Global SLR data, presented by Church and
258 White (2011), were used for that purpose due to a lack of reliable estimates of
259 local eustatic SLR.

260 Storm activity was parameterized by storm frequency, defined as the number of
261 tides above a certain storm level, and by storm intensity, defined as the mean
262 height of these storm tides. For storm parameterization, we used these definitions
263 in order to ensure that storm intensity is statistically independent from storm
264 frequency. Mean sea level in turn was calculated as a function of MHW and
265 MLW (Wahl et al., 2010).

266 Mean values of storm intensity and frequency data were aggregated for all years
267 in which an estimate for accretion rate was available, using a moving average
268 filter. Taking into account an expected error and temporal resolution of the dating
269 of the sediment layers, the window size was chosen to be 5 years.

270 **Analysis of storm-related salt marsh accretion**

271 One of the main objectives of this study is to investigate the influence of storm
272 frequency and storm intensity on the observed accretion rates. Multiple linear
273 regression analysis was employed to assess how much of the variation within the
274 accretion rate time series can be explained by one of these parameters. This
275 analysis was carried out by including all high water levels that flooded the marsh
276 from 1938-2007. By gradually increasing the storm level, and therefore excluding
277 the low inundation events, we investigated how different high water levels were
278 influencing accretion rates in the past. The standardized coefficients (β) of the
279 multiple linear regressions, as well as the p-values were compared for the different
280 storm levels.

281 **RESULTS**

282 **Grain size analysis and organic carbon content, and bulk density**

283 In each of the cores a fine-grained upper layer is underlain by layers comprised of
284 mainly coarse-grained sediments. The transition zone in core S1 is very distinct
285 and fine-grained sediments are not present below a depth of about 10 cm (Fig. 3).
286 In contrast, the transition zones in cores S2 and S3 are more gradual. Fine-grained
287 sediment is, in fact, present throughout the entire core S2 (Fig. 3).
288 Bulk densities reproduce this pattern of fine-grained sediments on top of a coarse-
289 grained base layer by increasing at the interfaces of salt marsh sediments and the
290 sandy base layer (Fig. 3). In core S1, a clear increase of bulk density is observed
291 at a depth of about 10 cm, reaching 1574 kg m^{-3} . The high bulk density of
292 1469 kg m^{-3} at the depth of 4.5 cm is considered as an outlier and was therefore
293 excluded from the analysis. Instead, the average from the neighboring upper and

294 lower layers was employed. The increase in S2 is more gradual and constant, with
295 a maximum bulk density of 939 kg dm^{-3} at 27 cm. In core S3, a considerable
296 increase in bulk density is observed at a depth of about 5 cm, with a maximum
297 value of 1591 kg m^{-3} . Within the silty salt marsh sediments bulk densities in cores
298 S2 and S3 do not significantly increase, mostly varying between 500 and
299 600 kg m^{-3} . In core S1 a significant increase from 326 to 656 kg m^{-3} within the
300 uppermost 6 cm is observed, bulk density then decreases to $450\text{-}500 \text{ kg m}^{-3}$ in the
301 lower silty layers.

302 Salt marsh sediments are characterized by fine-grained material with high organic
303 content, which allows for visual and experimental determination of the thickness
304 of the marsh layer deposited on top of the sandy base. Herein, the base of the
305 marsh can clearly be identified in cores S1 and S3 at 8.5 cm and 4.5 cm
306 respectively; whereas it is not as clear in core S2 (Fig. 3). The fine-grained
307 fraction rapidly decreases at 21 cm, but increases at 23 and 27 cm again. Although
308 high fractions of sand at depths of 21 and 25 cm are found, marsh development
309 seems to have started at a depth of about 27 cm.

310 The increase of bulk density within the uppermost 5 cm of core S1 was found to
311 fit the logarithmic model (equation 6; $R^2=0.97$, $p<0.02$), which is considered as
312 evidence for autocompaction. Model parameters A and B were estimated to be
313 0.0879 and 0.3791, respectively. The autocompaction rate during the growth of
314 the salt marsh therefore averages 1 mm yr^{-1} .

315 **Aerial photographs**

316 The first photograph available, taken in 1937 (Fig. 4a), provides strong evidence
317 for the presence of marsh at locations S1 and S2, however no marsh is yet present
318 at location S3. A sand bar seems to have formed between the seaward edge of the

319 marsh and the adjacent tidal flat. At the landward edge of the marsh sand appears
320 to be transported onto the marsh surface. However, in the following photograph
321 from 1958 (Fig. 4b), sand transport onto the marsh at the landward edge seems to
322 be less visible than in 1937; meanwhile the sand bar at the seaward edge has
323 developed further offshore. Recent photographs from 1988 and 1995 (Fig. 4c+d)
324 do not show considerable changes of the marsh extension towards the land, but do
325 indicate a seaward expansion. In 1988 (Fig. 4c), core location S3 is found to be in
326 a channel between the developing pioneer marsh and the mature main part of the
327 marsh. The photo from 1995 (Fig. 4d), shows that the channel appears to be
328 closed and covered by pioneer marsh vegetation. Marsh development at core
329 location S3 is, therefore, estimated to have started between 1988 and 1995.

330 **Radioisotope data**

331 *²¹⁰Pb data*

332 All three depth profiles of excess ²¹⁰Pb (²¹⁰Pb_{XS}) generally decrease as expected
333 (Fig. 5). Large variations are found in the surface concentrations, with the highest
334 activity (232 Bq kg⁻¹ in 1.5 cm) in core S1. Distinct peaks are found at a depth of
335 1.5 cm in all three cores.

336 In core S1 a slow decrease is observed, due to relatively high activities
337 (116 Bq kg⁻¹, 112 Bq kg⁻¹) at depths of 4.5 and 5.5 cm. Activities below 10 cm are
338 all less than the the detection limit and therefore less than 12.6 Bq kg⁻¹ (Fig. 5).

339 The initial decrease in S2 is much greater, and influenced by low activity at
340 4.5 cm (below detection limit of 9.5 Bq kg⁻¹). Activities below 4.5 cm decrease
341 slower, eventually resulting in activities below the detection limit for all depths
342 lower than 17 cm (Fig. 5). In core S3, ²¹⁰Pb_{XS} also quickly decreases within the

343 upper 7 cm from 129 Bq kg⁻¹ at 1.5 cm to less than 2.6 Bq kg⁻¹ at 7.5 cm. ²¹⁰Pb_{XS}
344 activities at lower depths are all below the detection limit (Fig. 5).

345 As ²¹⁰Pb activities in the sandy substrate of the cores S1 and S3 are all below the
346 detection limit, normalization for grain size and organic carbon content of these
347 activities is impossible. In core S2, where the fraction of fine grained, highly
348 organic sediment is rather constant within salt marsh layers, normalization is not
349 necessary.

350 ¹³⁷Cs data

351 ¹³⁷Cs peaks are found in cores S1 and S2. In core S3, no ¹³⁷Cs peak was found. S1
352 is characterized by a major peak at a depth of 5.5 cm (267 Bq kg⁻¹) and a minor
353 peak at 8.5 cm (38 Bq kg⁻¹; Fig. 6). ¹³⁷Cs appears to decrease towards zero at
354 about 15 cm, although it should be considered that the sediment below 10 cm is
355 very coarse and the effect of coarse grained sediment might reduce the ¹³⁷Cs-
356 activity (He and Walling, 1996a). In core S2 the situation is clearer: 2 peaks are
357 found in depths of 5.5 cm (64 Bq kg⁻¹) and 17 cm (52 Bq kg⁻¹); we note that the
358 upper peak's activity is significantly lower than the activity in S1 (Fig. 6). The
359 ¹³⁷Cs activity in core S3 is missing a distinct peak and has a very low activity
360 (<1 Bq kg⁻¹) in the sandy base layer. Finer sediments in the upper layers are
361 marked by a slight increase in activity up to 8 Bq kg⁻¹ (Fig. 6).

362 *Age of base layer*

363 The age of the marsh and the mean accretion rates were determined by
364 radioisotope dating (²¹⁰Pb) and compared with aerial photographs (table 1). The
365 base layer at core location S1 is found at a depth of about 8.5 cm (Fig. 2, 3).

366 Aerial photographs show that the marsh was present in 1937. However, analysis

367 of ^{210}Pb data does not support this finding, suggesting the marsh to be younger.
368 Several ^{210}Pb data in core S1 and S3 are below the detection limit due to a
369 relatively high baseline activity in these samples. Since the detection limit is
370 considered as a maximum activity and allows for activities within the range of
371 zero to the detection limit, the original error range needs to be extended. Therefore
372 the year when the base layer was deposited (according to ^{210}Pb dating) is
373 calculated to be between 1925 (± 5 years) and 1955 (± 5 years) (table 1). Utilizing
374 these dates and the aerial photographic evidence we conclude that the marsh
375 started to develop between 1925 (± 5 years) and 1937, resulting in a mean
376 accretion rate between 1 and 1.2 mm yr^{-1} . In core S2 the base layer is found at a
377 depth of 27 cm (Fig. 2, 3). ^{210}Pb dating suggests that this layer was deposited in
378 1915 (± 5 years). The aerial photograph of 1937 confirms the existence of the
379 marsh at that time. Therefore, the mean accretion rate for core location S2 is
380 estimated to be 2.8 mm yr^{-1} (table 1). S3 has a marsh layer that is only 4.5 cm
381 thick (Fig. 2, 3), but no ^{210}Pb measurement is available for the base layer at that
382 depth. Meanwhile the sample at 3.5 cm is calculated to be deposited in 1996,
383 suggesting a mean accretion rate of 2.5 mm yr^{-1} . Aerial photographs indicate the
384 beginning of the pioneer (*Spartina*-) marsh development between 1988 and 1995.

385 *Accretion rates*

386 A reliable time series of accretion rates could only be drawn for the core S2,
387 because the marsh layer in S3 is too thin to show significant variations, while
388 ^{210}Pb dating for S1 resulted in small accretion rates associated with large
389 uncertainties. However, for S1, a general trend towards an increase of accretion
390 rates can be observed from the beginning of the 1960s, resulting in a recent
391 accretion rate between 3 and 3.5 mm yr^{-1} . Accretion rates for S2 indicate strong

392 variations over the last 75 years, ranging from about 1 mm yr⁻¹ up to 16 mm yr⁻¹
393 (Fig. 7). No clear trend can be observed, although accretion rates in the 1980's
394 and 1990's seem to be higher. Two distinct peaks are found in 1982 and 1992
395 (according to ²¹⁰Pb dating).

396 **Hydrology and meteorology**

397 Tide gauge data from 1938 to 2007 were analyzed for historic trends (Fig. 8) and
398 compared to ²¹⁰Pb-derived marsh elevations (Fig. 9). It is shown that the MSL at
399 the tide gauge *Hoernum Hafen* within that time period rose by about 2.1 mm yr⁻¹,
400 slightly greater than the global rate of SLR of 1.8 mm yr⁻¹ during the same period
401 (Church and White, 2011). The rise of MSL was accompanied by a mean increase
402 of the MHW of about 4 mm yr⁻¹, while the MLW did not change significantly.
403 The increase of both MHW and MSL was observed to accelerate since about the
404 early 1980's. This corresponds to data analyzed by Wahl et al. (2010), who further
405 pointed out that SLR rates during the last 10-15 years within the German Bight
406 were higher than the global average, as reported by Church et al. (2008). The
407 frequency of storm floods was analyzed based on their definition given by the
408 German Maritime and Hydrographic Agency (BSH), where storm floods are
409 water levels exceeding 1.5 m above MHW. Considering that the averaged yearly
410 MHW from 1938 to 2007 is 0.9 m above NN, this corresponds to a storm level of
411 2.4 m NN. It was shown that storm frequency experienced a linear increase of
412 0.06 events yr⁻¹, while 1984 and 1990 were marked by the greatest number of
413 storms with 10 and 11 events, respectively. During the same period the intensity
414 of these storms did not significantly change.
415 As MHW increased rapidly within the last 50 years, salt marsh growth was not
416 able to keep pace with this rise. An average of 2.6 and 1.3 mm yr⁻¹ was lost

relative to MHW at core location S1 and S2 respectively. Core location S3 was observed to accrete at a rate of 2.5 mm yr^{-1} since 1996. Meanwhile, during that period, MHW strongly increased with a rate of 11 mm yr^{-1} (Fig. 9). Marsh elevation of S2 relative to MSL, on the other hand increased by 0.7 mm yr^{-1} , while S1 decreased by 0.6 mm yr^{-1} (Fig. 9).

Influence of storm frequency and intensity on accretion rates

The marsh at core location S2 floods when the water level reaches 134 cm (NN; Fig. 2). Multiple linear regression analysis shows that storm intensity ($\beta=0.88$, $p<0.01$) describes accretion rates better than storm frequency ($\beta=0.06$, $p>0.1$), when considering all inundation events (Fig. 10). However, with an increasing maximum storm level there is a decreasing influence of the storm intensity, whereas the influence of storm frequency gradually increases. At a storm level of 260 cm, for example, storm frequency gives a β of 0.86 ($p<0.01$), while storm intensity cannot explain accretion rates significantly ($\beta=0.04$, $p>0.1$; Fig. 11). It appears that the storm level of 152 cm (equals an inundation height of 18 cm at core location S2) is the turning point where the influence of storm frequency becomes statistically significant ($p<0.1$); meanwhile the influence of storm intensity progressively diminishes (Fig. 12).

DISCUSSION

^{210}Pb geochronologies were used at three salt marsh levels (i) to determine the age of the marsh and to reconstruct its evolution, (ii) to assess temporal variations of accretion rates at all three core locations, and (iii) to identify the hydrological parameters influencing marsh accretion.

440 **Support for accretion rate calculation**

441 In contrast to the continuous deposition of ^{210}Pb on the marsh surface, ^{137}Cs serves
442 as a marker horizon that can be used to calculate mean accretion rates in between
443 the years 1963, 1986, and 2009, when the cores were extracted. It is, therefore, an
444 additional independent geochronometer that allows for comparison with the ^{210}Pb
445 dating method, but not for derivation of higher resolved temporal accretion rates.
446 Both the 1963 and 1986 peaks were found in cores S1 and S2. In core S1, ^{137}Cs
447 overestimates accretion rates compared to the ^{210}Pb data and the aerial photograph
448 of 1937 (Fig. 9). It seems that ^{137}Cs has been transported further down in the soil
449 column, although we are not certain of the mechanism. A very good agreement
450 between the three methods (^{137}Cs , ^{210}Pb , and aerial photographs) is found in core
451 S2 and in core S3. ^{137}Cs in core S2 shows two distinct peaks at depths of 5.5 cm
452 and 17 cm. ^{210}Pb dating is supported by these peaks; the layers at depths of 5.5 cm
453 and 17 cm were estimated to be deposited in 1992 and 1961 respectively (Fig. 9).
454 The absence of a peak in core S3 also supports what we can observe in the aerial
455 photographs, as well as the ^{210}Pb dating suggesting that the marsh development
456 started after 1988.

457 Grain size data also support the ^{210}Pb dating in core S2 to a certain degree. Two
458 layers (5.5 cm and 9.5 cm) show an elevated fraction of coarse-grained sediments
459 in comparison to the other layers (Fig. 3). ^{210}Pb dating calculates that these layers
460 were deposited in 1992 (± 5 years) and 1985 (± 5 years). In 1990, the highest
461 number of storms occurred during the last 70 years (Fig. 8), 2 of which were
462 among the 5 most severe storm surges (measured at *Hörnnum Hafen*) in recorded
463 history. Meanwhile, the year 1984 was marked by the second most frequent storm
464 events during the last 70 years (Fig. 8). We expect that the higher energy of

465 storms allows for the transport of coarser-grained materials onto the marsh by
466 both waves and currents.

467 **Mean accretion rates**

468 The spatial pattern of mean accretion rates shows a decrease from the low marsh
469 towards the inner marsh (table 1). This is a typical spatial phenomenon observed
470 on many marshes by various authors (Bartholdy et al., 2004; Cahoon and Reed,
471 1995; French and Spencer, 1993; Pethick, 1981; Temmerman et al., 2003a).
472 Meanwhile the mean accretion rate for the pioneer marsh zone is lower than the
473 one in the low marsh zone. Resuspension of sediment during the early stage of the
474 marsh development could be the reason for this pattern. The measured accretion
475 rates generally compare well with mean accretion rates measured on the peninsula
476 of Skallingen, where Bartholdy et al. (2004) found the accretion rate on the
477 Skallingen marsh to vary between 2 mm yr⁻¹ on the inner marsh and 4 mm yr⁻¹ on
478 the outer marsh. Measurements of Kirchner and Ehlers (1998) in the eastern part
479 of Sylt, however, have shown much higher accretion rates between 5.8 mm yr⁻¹
480 and 15.2 mm yr⁻¹, but grain sizes in this section of Sylt are much finer, indicating
481 different hydrodynamic conditions favoring settling of sediment.

482 **Temporal variations of accretion rates**

483 S2 shows strong temporal variations of accretion with a period of higher rates
484 found during the 1980s and 1990s including two distinct peaks in 1982 and 1992
485 and a rapid decrease in accretion rates during the last 20 years. This pattern
486 strongly resembles the periods of high storm activity (Fig. 10, 11). Although
487 temporal variations of accretion rates in S1 should only be considered as an
488 approximation, a trend towards increasing accretion rates to current values

489 between 3-3.5 mm yr⁻¹ is observed. The few data points that exist for S3 show a
490 constant accretion rate of 2.5 mm yr⁻¹.

491 Accretion rates at core location S2 during calm periods seem to lie close to the
492 rates of eustatic SLR (Fig. 10, 11), while, during stormy years, accretion rates are
493 much higher than SLR. This behavior shows the importance of storms for the
494 resilience of salt marshes towards eustatic SLR. Even though, accretion rates
495 during calm years are still sufficiently high, a considerable decrease in storminess
496 would lower the marsh elevation and possibly affect the marsh zonation.

497 **Historic development of the marsh**

498 Using the data presented in the previous section it is possible to reconstruct the
499 historic evolution of the marsh: Marsh development at our study site seems to
500 have started after about 1915. Prior to marsh development, we assume a bare
501 sandy beach slope at that location. The age of the base layer at core location S2
502 indicates that marsh development started during a period of rapidly increasing
503 MHW and MLW levels (Jensen and Mudersbach, 2004; Wahl et al., 2010).
504 Increasing inundation frequencies may have triggered the development of pioneer
505 marsh vegetation, such as *Salicornia* and *Suaeda*, probably sheltered by a seaward
506 sandy ridge. At some point, the sandy ridge at the seaward edge moved offshore
507 and a cliff arose due to increased hydrodynamics caused by more frequent
508 inundation events. As a consequence, a channel developed in front of the marsh,
509 which probably acted as a tidal channel, building up levees at the landward and
510 seaward side (Pedersen and Bartholdy, 2007). According to the aerial photograph
511 in 1988, the pioneer marsh started to develop on top of the sand bar and slowly
512 spread towards the cliff at the marsh edge, stabilizing the latter. Decreased
513 hydrodynamics in the vicinity of the sand bar, a constantly low MLW-level, and a

514 spread of the invasive species *Spartina anglica* after 1987 (Loebl et al., 2006),
515 may have triggered that process. Today the cliff is located far inside the marsh
516 and the pioneer marsh seems to expand further onto the tidal flat and accrete faster
517 than MSLR.

518 The inner part of the marsh accreted with the slowest overall accretion rate. While
519 the base layer is approximately 30 cm above the base layer in the central part of
520 the marsh, marsh development started between 1925 and 1937. During the first
521 few decades of growth, aerial photographs indicate that considerable amounts of
522 sand may have been blown onto this part of the marsh; although, accretion rates
523 were too low to detect significant temporal variations. The topography of the
524 marsh platform has been flattened during the last 75 years due to higher accretion
525 rates in the middle of the marsh, than on the landward side of the marsh.

526 **Influence of storms on accretion**

527 The analysis presented in this study focuses on the historical vertical development
528 of a single salt marsh. It is shown that an increase of storminess positively
529 correlates with marsh accretion rates. While many authors have focused on the
530 destructive, erosional influence of storms on salt marshes (e.g. Callaghan et al.
531 2010, Mariotti and Fagherazzi 2010, van de Koppel et al. 2005), our methods are
532 not able to reproduce the lateral marsh development and their implications on
533 accretion processes, but rather the vertical marsh accretion.

534 Vertical accretion (at core location S2) was shown to be closely linked to past
535 storm patterns with accretion rates of up to 16 mm yr⁻¹ in very stormy years.

536 Linear regression analysis showed that both storm intensity and storm frequency
537 are important factors influencing accretion rates. Storm frequency does not seem
538 to be the driving factor of accretion if storm levels do not rise higher than 18 cm

539 above the marsh surface at S2. The importance of frequency greatly increases
540 above this threshold level (Fig. 12). We hypothesize that the presence and the
541 height of the vegetation could be the reason for this threshold.

542 Assuming that the threshold value we found for the core S2 is true for different
543 marsh elevations as well, we can identify two different driving factors for marsh
544 accretion in the lower and the higher parts of the marsh: In the lower marsh zones,
545 where inundation is frequent and usually higher than the vegetation height,
546 accretion rates increase with increasing inundation frequency. Inundation
547 frequency at low elevations, in turn, is highly correlated with the MHW level and
548 possibly caused by SLR. In the higher parts of the marsh, where inundation is less
549 frequent and heights of the inundation are often lower or just slightly higher than
550 the vegetation height, we expect the mean strength of the storms to be more
551 important than the actual number of storms.

552 These findings are especially relevant when considering possible implications on
553 storm related accretion processes. Assuming that more sediment is in suspension
554 when storm water levels are high, the solution of the mass balance equation for
555 incoming and settling sediment (Mudd et al., 2010; Temmerman et al., 2003a)
556 results in an exponential increase of accretion rates with higher storm water levels
557 (Fig. 13; Temmerman et al., 2003a). Considering our results, the effect of storm
558 intensity on salt marsh accretion is suggested to be stronger at low storm water
559 levels than at high storm water levels, resulting in a logarithmic rather than an
560 exponential relationship between storm water levels and accretion rates (Fig. 13).

561 The height at which the logarithmic curve starts to flatten is hypothesized to be
562 connected to the height of the vegetation. Vegetation has a strong effect on flow
563 velocities and the Reynolds number within the vegetation canopy and can
564 therefore influence the flocculation and break-up processes of the sediment in

suspension (Winterwerp, 2002). Low flow velocities within the vegetation canopy could therefore result in larger floc sizes and corresponding settling velocities, while high flow velocities could decrease the floc sizes and decrease the settling velocities of the sediment particles (Bartholomä et al., 2009). This would infer that the depth-averaged settling velocity would decrease with inundation heights that exceed the vegetation height and result in a flattening of the above mentioned curve. We must emphasize that this hypothesis should be further investigated by explicitly examining flocculation processes over salt marsh surfaces during storm events.

Conclusions

In accordance with the available literature, ^{210}Pb has proven to be a good tool for determination of sediment accretion rates on salt marshes. ^{137}Cs data and aerial photographs independently supported the ^{210}Pb dating and the derived accretion rates. However, restrictions and limitation of the method can be recognized in core S1 and S3. Based on the results of this study we make the following conclusions:

- (1) While not always coincident with one another, both storm frequency and intensity seem to affect salt marsh accretion rates. In very stormy years, accretion rates can increase 5-fold above mean value. Frequent and strong storms have shown that they can lead to accretion rates which are higher than MSLR and, therefore are considered as an important factor for the ability of marshes to keep pace with eustatic SLR.
- (2) We show that eustatic SLR slightly increases accretion rates during calm wind periods, while a surplus of accretion is observed in stormy years, leading to a net increase of marsh elevation relative to mean sea level,

590 accompanied by a slight decrease in elevation relative to the more rapidly
591 rising mean tidal high water level.

592 (3) There exists a threshold for inundation depth (18 cm) on the investigated
593 marsh at which the relative importance of storm frequency and intensity
594 reverses. Storm intensity seems to be the driving factor for high accretion
595 rates below an inundation depth of 18 cm, while storm frequency is more
596 important above this inundation depth. The influence of vegetation is
597 suggested to be the reason for this threshold.

598 (4) The existence of a threshold for inundation depth implies that accretion of
599 higher marsh zones is crucially dependent on the storm intensity, while lower
600 marsh parts rather depend on the development of storm frequency and mean
601 high water level, possibly influenced by a mean sea level rise. The different
602 major driving factors for the marsh zones may lead to changes in marsh
603 zonation, if storm activity and SLR rate change in the future.

604 Further investigation, including short-term measurements of accretion rates during
605 storm events and modeling is necessary to better understand the singular effects of
606 storm intensity, storm frequency, and sea level rise on accretion processes. Also,
607 more marshes in mesotidal environments need to be investigated to test whether a
608 similar critical inundation depth threshold exists elsewhere and the hypothesis of
609 vegetation being responsible can be verified.

610 **Acknowledgements**

611 This project was funded by the Cluster of Excellence 80 “The Future Ocean”. The
612 „Future Ocean“ is funded within the framework of the Excellence Initiative by the
613 Deutsche Forschungsgemeinschaft (DFG) on behalf of the German federal and

614 state governments. Furthermore we would like to thank Anton Eisenhower for his
 615 support and the 'Laboratory for Radioisotopes' in Goettingen for running the
 616 radiometric measurements. For their help in the field and during the preparation of
 617 the samples, we thank Daniela Arp, Michal Lichter, Tina Geissler, Natalia
 618 Zamora, and Claudia Wolff. The hydrological data for the tide gauge Hörnum
 619 Hafen were kindly supplied by Thomas Wahl, Jacobus Hofstede, and Gerd
 620 Hartwig. We would also like to thank the two anonymous reviewers for their
 621 valuable comments, which have helped in improving this manuscript.

622 **References**

- 623 Ahrendt, K. and R. Köster. 1998. Sylt - einst und jetzt. In *Umweltatlas Wattenmeers, Band 1,*
 624 *Nordfriesisches und Dithmarscher Wattenmeer*, eds. Nationalpark Schleswig-Holsteinisches
 625 *Wattenmeer (Tönning) and Umweltbundesamt (Berlin)*, 38-39. Stuttgart: Eugen Ulmer.
- 626 Ahrendt, K. and J. Thiede. 2001. *Naturräumliche Entwicklung Sylts - Vergangenheit und Zukunft.*
 627 *In Sylt - Klimafolgen für Mensch und Küste*, eds. Daschkeit A. and P. Schottes, 69-112. Berlin:
 628 Springer.
- 629 Allen, J. R. L. 2000. Morphodynamics of Holocene salt marshes: a review sketch from the Atlantic
 630 and Southern North Sea coasts of Europe. *Quaternary Science Reviews* 19:1155-1231.
- 631 ALW - Amt für Land- und Wasserwirtschaft Husum. 1997. *Fachplan Küstenschutz Sylt -*
 632 *Fortschreibung*. Husum.
- 633 Andersen, T. J., O. A. Mikkelsen, A. L. Møller, and P. Morten. 2000. Deposition and mixing
 634 depths on some European intertidal mudflats based on ²¹⁰Pb and ¹³⁷Cs activities. *Continental*
 635 *Shelf Research* 20:1569-1591.
- 636 Appleby, P. G. and F. Oldfield. 1978. The calculation of lead-210 dates assuming a constant rate of
 637 supply of unsupported ²¹⁰Pb to the sediment. *Catena* 5:1-8.
- 638 Appleby, P. G. and F. Oldfield. 1983. The assessment of ²¹⁰Pb data from sites with varying
 639 sediment accumulation rates. *Hydrobiologia* 103:29-35.
- 640 Armentano, T. V. and G. M. Woodwell. 1975. Sedimentation Rates in a Long Island Marsh
 641 Determined by ²¹⁰Pb Dating. *American Society of Limnology and Oceanography* 20:452-456.

642 Bartholdy, J., C. Christiansen, and H. Kunzendorf. 2004. Long term variations in backbarrier salt
 643 marsh deposition on the Skallingen peninsula - the Danish Wadden Sea. *Marine Geology* 203:1-
 644 21.
 645 Bartholdy, J., J. B. T. Pedersen, and A. T. Bartholdy. 2010. Autocompaction of shallow silty salt
 646 marsh clay. *Sedimentary Geology* 223:310-319.
 647 Bartholomä, A., A. Kubicki, T. Badewien, and B. Flemming. 2009. Suspended sediment transport
 648 in the German Wadden Sea—seasonal variations and extreme events. *Ocean Dynamics* 59:213-
 649 225.
 650 Bellucci, L. G., M. Frignani, J. K. Cochran, S. Albertazzi, L. Zaggia, G. Cecconi, and H. Hopkins.
 651 2007. Pb-210 and Cs-137 as chronometers for salt marsh accretion in the Venice Lagoon - Links to
 652 flooding frequency and climate change. *Journal of Environmental Radioactivity* 97:85-102.
 653 Beniston, M., D. Stephenson, O. Christensen, C. Ferro, C. Frei, S. Goyette, K. Halsnaes, T. Holt,
 654 K. Jylhä, B. Koffi, J. Palutikof, R. Schöll, T. Semmler, and K. Woth. 2007. Future extreme events
 655 in European climate: an exploration of regional climate model projections. *Climatic Change* 81:71-
 656 95.
 657 BSH - Bundesamt für Seeschifffahrt und Hydrographie. 2008. *Gezeitentafeln 2009 - Europäische*
 658 *Gewässer*. Hamburg and Rostock: BSH.
 659 Cahoon, D. R. and D. J. Reed. 1995. Relationships among Marsh Surface Topography,
 660 Hydroperiod, and Soil Accretion in a Deteriorating Louisiana Salt Marsh. *Journal of Coastal*
 661 *Research* 11:357-369.
 662 Callaghan, D. P., T. J. Bouma, P. Klaassen, D. Van der Wal, M. J. F. Stive, and P. M. J. Herman.
 663 2010. Hydrodynamic forcing on salt-marsh development: Distinguishing the relative importance
 664 of waves and tidal flows. *Estuarine, Coastal and Shelf Science* 89:73-88.
 665 Chmura, G. L., A. Coffey, and R. Crago. 2001. Variation in surface sediment deposition on salt
 666 marshes in the Bay of Fundy. *Journal of Coastal Research* 17:221-227.
 667 Church, J. and N. White. 2011. *Sea-Level Rise from the Late 19th to the Early 21st Century*.
 668 *Surveys in Geophysics*:1-18.
 669 Church, J., N. White, T. Aarup, W. Wilson, P. Woodworth, C. Domingues, J. Hunter, and K.
 670 Lambeck. 2008. Understanding global sea levels: past, present and future. *Sustainability Science*
 671 3:9-22.

672 Compton, A. H. 1923. A Quantum Theory of the Scattering of X-rays by Light Elements. *Physical*
673 *Review* 21:483-502.

674 De Groot, A. 2009. Salt-marsh sediment: Natural γ -radioactivity and spatial patternsthesi,
675 University of Groningen.

676 Delaune, R. D., W. H. Patrick, and R. J. Buresh. 1978. Sedimentation rates determined by ^{137}Cs
677 dating in a rapidly accreting salt marsh. *Nature* 275:532-533.

678 Dijkema, K. S. 1987. Geography of Salt Marshes in Europe. *Zeitschrift Fur Geomorphologie*
679 31:489-499.

680 Fischer-Bruns, I., H. Storch, J. González-Rouco, and E. Zorita. 2005. Modelling the variability of
681 midlatitude storm activity on decadal to century time scales. *Climate Dynamics* 25:461-476.

682 French, J. 2006. Tidal marsh sedimentation and resilience to environmental change: Exploratory
683 modelling of tidal, sea-level and sediment supply forcing in predominantly allochthonous systems.
684 *Marine Geology* 235:119-136.

685 French, J. R. 1993. Numerical simulation of vertical marsh growth and adjustment to accelerated
686 sea-level rise, North Norfolk, U.K. *Earth Surface Processes and Landforms* 18:63-81.

687 French, J. R. and T. Spencer. 1993. Dynamics of sedimentation in a tide-dominated backbarrier
688 salt marsh, Norfolk, UK. *Marine Geology* 110:315-331.

689 Goodbred, S. L. and S. A. Kuehl. 1998. Floodplain processes in the Bengal Basin and the storage
690 of Ganges-Brahmaputra river sediment: an accretion study using ^{137}Cs and ^{210}Pb geochronology.
691 *Sedimentary Geology* 121:239-258.

692 Harrison, E. Z. and A. L. Bloom. 1977. Sedimentation rates on tidal salt marshes in Connecticut.
693 *JOURNAL OF SEDIMENTARY RESEARCH* 47:1484-1490.

694 He, Q. and D. E. Walling. 1996a. Interpreting particle size effects in the adsorption of ^{137}Cs and
695 unsupported ^{210}Pb by mineral soils and sediments. *Journal of Environmental Radioactivity*
696 30:117-137.

697 He, Q. and D. E. Walling. 1996b. Use of fallout Pb-210 measurements to investigate longer-term
698 rates and pattern of overbank sediment deposition on the floodplains of lowland rivers. *Earth*
699 *Surface Processes and Landforms* 21:141-154.

700 Hildebrandt, V., J. Gemperlein, U. Zeltner, and W. Peteresen. 1993. Landesweite Biotopkartierung
701 - Kreis Nordfriesland: Landschaftsentwicklung - Aktuelle Situation - Flächenschutz. Kiel:
702 Landesamt für Naturschutz und Landschaftspflege Schleswig-Holstein.

703 Jensen, J. and C. Muddersbach. 2004. Zeitliche Änderungen in den Wasserstandszeitreihen an den
 704 Deutschen Küsten. In *Klimaänderung und Küstenschutz, Conference Proceedings*, eds. Gönner
 705 G., H. Grassl, D. Kelletat, H. Kunz, B. Probst, H. von Storch, and J. Sündermann, 115-128.
 706 Hamburg.
 707 Kelletat, D. 1992. Coastal Erosion and Protection Measures at the German North Sea Coast.
 708 *Journal of Coastal Research* 8:699-711.
 709 Kirchner, G. and H. Ehlers. 1998. Sediment Geochronology in Changing Coastal Environments:
 710 Potentials and Limitations of the ^{137}Cs and ^{210}Pb Methods. *Journal of Coastal Research* 14:483-
 711 492.
 712 Kirwan, M. and S. Temmerman. 2009. Coastal marsh response to historical and future sea-level
 713 acceleration. *Quaternary Science Reviews* 28:1801-1808.
 714 Kirwan, M. L. and G. R. Guntenspergen. 2010. Influence of tidal range on the stability of coastal
 715 marshland. *Geophysical Research Letters* 115:F02009.
 716 Kirwan, M. L., G. R. Guntenspergen, A. D'Alpaos, J. T. Morris, S. M. Mudd, and S. Temmerman.
 717 2010. Limits on the adaptability of coastal marshes to rising sea level. *Geophysical Research*
 718 *Letters* 37:L23401.
 719 Koide, M., A. Soutar, and E. D. Goldberg. 1972. Marine geochronology with ^{210}Pb . *Earth and*
 720 *Planetary Science Letters* 14:442-446.
 721 Kolker, A. S., S. L. Goodbred Jr, S. Hameed, and J. K. Cochran. 2009. High-resolution records of
 722 the response of coastal wetland systems to long-term and short-term sea-level variability.
 723 *Estuarine, Coastal and Shelf Science* 84:493-508.
 724 Kunzendorf, H., K.-C. Emeis, and C. Christiansen. 1998. Sedimentation in the Central Baltic Sea
 725 as Viewed by Non-Destructive Pb-210-dating *Geografisk Tidsskrift* 98:1-8.
 726 Loebl, M., J. Beusekom, and K. Reise. 2006. Is spread of the neophyte *Spartina anglica* recently
 727 enhanced by increasing temperatures? *Aquatic Ecology* 40:315-324.
 728 Malvern Instruments Ltd. 2010. Mastersizer 2000.
 729 <http://www.malvern.de/LabGer/products/Mastersizer/MS2000/mastersizer2000.htm>. Accessed 31
 730 August 2010.
 731 Mariotti, G. And S. Fagherazzi. 2010. A numerical model for the coupled long-term evolution of
 732 salt marshes and tidal flats. *Journal Geophysical Research* 115:F01004.

733 Milne, G. A., A. J. Long, and S. E. Bassett. 2005. Modelling Holocene relative sea-level
 734 observations from the Caribbean and South America. *Quaternary Science Reviews* 24:1183-1202.
 735 Möller, I. 2006. Quantifying saltmarsh vegetation and its effect on wave height dissipation:
 736 Results from a UK East coast saltmarsh. *Estuarine, Coastal and Shelf Science* 69:337-351.
 737 Mudd, S. M., A. D'Alpaos, and J. T. Morris. 2010. How does vegetation affect sedimentation on
 738 tidal marshes? Investigating particle capture and hydrodynamic controls on biologically mediated
 739 sedimentation. *Journal of Geophysical Research* 115:F03029.
 740 Nikulina, A. 2008. The imprint of anthropogenic activity versus natural variability in the fjords of
 741 Kiel Bight: Evidence from Sediments. PhD thesis, University of Kiel.
 742 Orson, R., W. Panageotou, and S. P. Leatherman. 1985. Response of Tidal Salt Marshes of the
 743 U.S. Atlantic and Gulf Coasts to Rising Sea Levels. *Journal of Coastal Research* 1:29-37.
 744 Pedersen, J. B. T. and J. Bartholdy. 2007. Exposed salt marsh morphodynamics: An example from
 745 the Danish Wadden Sea. *Geomorphology* 90:115-125.
 746 Pedersen, J. B. T., J. Bartholdy, and C. Christiansen. 2007. ¹³⁷Cs in the Danish Wadden Sea:
 747 contrast between tidal flats and salt marshes. *Journal of Environmental Radioactivity* 97:42-56.
 748 Pethick, J. S. 1981. Long-term accretion rates on tidal salt marshes. *Journal of Sedimentary*
 749 *Research* 51:571-577.
 750 Redfield, A. C. 1972. Development of a New England Salt Marsh. *Ecological Monographs*
 751 42:201-237.
 752 Reed, D. J. 1995. The response of coastal marshes to sea-level rise: Survival or submergence?
 753 *Earth Surface Processes and Landforms* 20:39-48.
 754 Reise, K., M. Baptist, B. P., N. Dankers, L. Fischer, B. Flemming, A. P. Oost, and C. Smit. 2010.
 755 The Wadden Sea - A Universally Outstanding Tidal Wetland. *Wadden Sea Ecosystem* 29.
 756 Common Wadden Sea Secretariat, Wilhelmshaven, Germany: 7-24.
 757 Rockel, B. and K. Woth. 2007. Extremes of near-surface wind speed over Europe and their future
 758 changes as estimated from an ensemble of RCM simulations. *Climatic Change* 81:267-280.
 759 Temmerman, S., G. Govers, P. Meire, and S. Wartel. 2003a. Modelling long-term tidal marsh
 760 growth under changing tidal conditions and suspended sediment concentrations, Scheldt estuary,
 761 Belgium. *Marine Geology* 193:151-169.

762 Temmerman, S., G. Govers, S. Wartel, and P. Meire. 2003b. Spatial and temporal factors
 763 controlling short-term sedimentation in a salt and freshwater tidal marsh, Scheldt estuary,
 764 Belgium, SW Netherlands. *Earth Surface Processes and Landforms* 28:739-755.
 765 The Trilateral Monitoring and Assessment Program - TMAP. 2006. Ubgkal07: Topographie DK
 766 und SH. Nationalpark Schleswig-Holsteinisches Wattenmeer. [http://www.waddensea-](http://www.waddensea-secretariat.org/TMAP/Data-Unit/Data.html)
 767 [secretariat.org/TMAP/Data-Unit/Data.html](http://www.waddensea-secretariat.org/TMAP/Data-Unit/Data.html). Accessed 20 November 2008
 768 van de Koppel, J., D. van der Wal, J. P. Bakker, and P. M. J. Herman. 2005. Self-organization and
 769 vegetation collapse in salt marsh ecosystems. *American Naturalist* 165:E1-E12.
 770 von Storch, H. and R. Weisse. 2008. Regional storm climate and related marine hazards in the
 771 Northeast Atlantic. In *Climate Extremes and Society*, eds. Diaz H. F. and R. J. Murnane, 54-73.
 772 Cambridge: Cambridge University Press.
 773 Wahl, T., J. Jensen, and T. Frank. 2010. On analysing sea level rise in the German Bight since
 774 1844. *Natural Hazards and Earth System Sciences* 10:171-179.
 775 Walling, D. E., A. L. Collins, and H. M. Sickingabula. 2003. Using unsupported lead-210
 776 measurements to investigate soil erosion and sediment delivery in a small Zambian catchment.
 777 *Geomorphology* 52:193-213.
 778 Williams, H. 2003. Modeling Shallow Autocompaction in Coastal Marshes Using Cesium-137
 779 Fallout: Preliminary Results from the Trinity River Estuary, Texas. *Journal of Coastal Research*
 780 19:180-188.
 781 Winterwerp, J. C. 2002. On the flocculation and settling velocity of estuarine mud. *Continental*
 782 *Shelf Research* 22:1339-1360.
 783 Woth, K., R. Weisse, and H. von Storch. 2006. Climate change and North Sea storm surge
 784 extremes: an ensemble study of storm surge extremes expected in a changed climate projected by
 785 four different regional climate models. *Ocean Dynamics* 56:3-15.
 786 WSA - Wasser- und Schifffahrtsamt Tönning. 2007. Wasserstandsinformationen: Hörnum/Sylt.
 787 <http://www.wsv.de/wsa-toe/service/wasserstandinfo/index.html>. Accessed 27 August 2010.
 788

789 TABLES

790 Table 1: Ages of base layers and mean sedimentation rates: Comparison of ^{210}Pb datings with
791 information from aerial photographs.

Core name	Depth of base layer	Age of base layer (^{210}Pb)	Age of base layer (aerial photographs)	Sedimentation rate (mm/year)
S1	8.5cm	1925-1955	<1937	1-1.2
S2	27	1915	<1937	2.8
S3	4.5cm	No measurement	1988-1995	2.5 (since 1996)

792 FIGURE LEGENDS

793 **Fig. 1:** The study area is located in the southeastern North Sea (cell 1), in the southern part of the
794 island of Sylt (cell 2). The cores were taken on a transect in three dominant vegetation zones,
795 indicated by points (cell 3).

796 **Fig. 2:** Topographic profile and marsh zonation of the investigated salt marsh. Core locations and
797 the sandy base layer are indicated by triangles and a dashed line respectively.

798 **Fig. 3:** Grain size composition (%) and bulk density calculations (kg m^{-3}), as described in equation
799 5, for all 3 cores and all depths (cm) that were measured. Grain size composition is depicted in the
800 bar graph and bulk density by the line graph. The depth of the sandy base layer is indicated by the
801 dashes line.

802 **Fig 4:** Aerial photographs of the investigated salt marsh from 1937 (a), 1958 (b), 1988 (c), and
803 1995 (d). Dark colours indicate vegetated areas. Bright colours indicate sand. Source:
804 Landesbetrieb für Küstenschutz, Nationalpark und Meeresschutz Schleswig-Holstein (LKN-SH)

805 **Fig. 5:** Excess ^{210}Pb (Bq kg^{-1}) in all three cores and all depths (cm) that were measured. Horizontal
806 error bars indicate propagated errors for excess ^{210}Pb . Measurements without horizontal error bars
807 were measured below detection limit. Vertical error bars represent the thickness of the measured
808 layer.

809 **Fig. 6:** ^{137}Cs (Bq kg^{-1}) in all three cores and all depths (cm) that were measured. Horizontal error
810 bars indicate measurement errors of ^{137}Cs . Vertical error bars represent the thickness of the
811 measured layer.

812 **Fig. 7:** Marsh sedimentation rates from 1938-2003 (mm yr^{-1}). Horizontal error bars represent the
813 averaged uncertainty of the ^{210}Pb dating.

814 **Fig. 8:** Hydrological data from 1938-2007 at tide gauge Hörnum Hafen (Sylt). Storm intensity
815 (stars), mean tidal high water (MHW), mean sea level (MSL), and mean tidal low water (MLW)
816 are given in meter above ‘Normal Null’ (NN). A 19-years running mean is given for MHW, MSL,
817 and MLW. Storm frequency (bars) is the number of storm events that exceeded the level of 2.4 m
818 above NN. Source: Wahl 2010, Hartwig 2010.

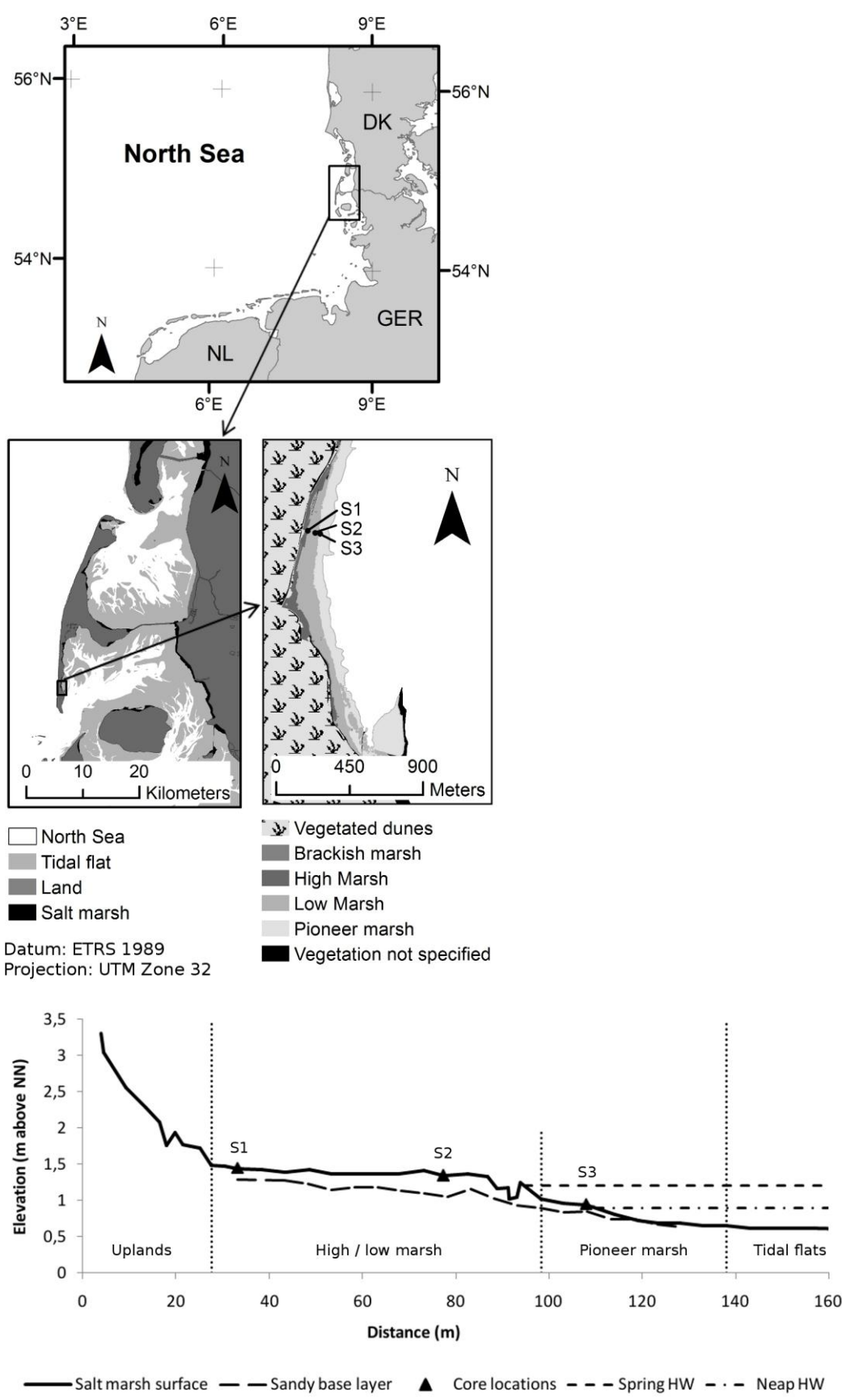
819 **Fig. 9:** Historic marsh elevations for all three cores derived from ^{210}Pb and ^{137}Cs data. Due to
820 several data points below the detection limit in core S1, two graphs are displayed, comparing the
821 fastest possible accretion rates (open circles) with the slowest possible accretion rates (filled
822 circles). For validation of the data, the ^{137}Cs peaks are included (open diamonds). The error bars
823 (as shown in figure 6) were omitted for clarity. The mean high water and the mean sea level
824 (MHW and MSL: solid lines) are displayed as 5-years running averages.

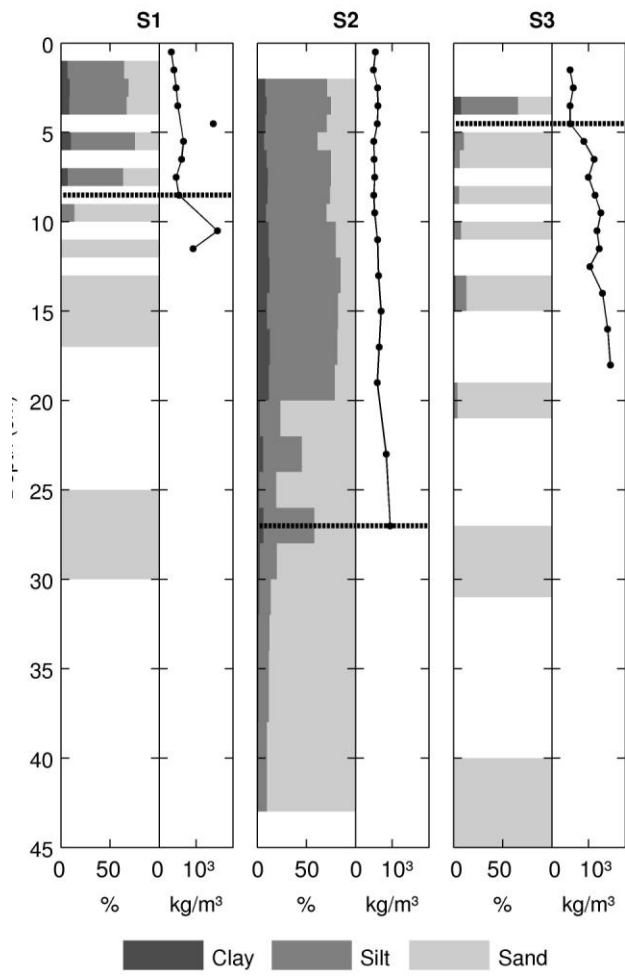
825 **Fig. 10:** Comparison of sedimentation rates (stars) at core location S2 with storm intensity (open
826 circles), defined as the mean height for all high water levels exceeding 1.34 m (NN).

827 **Fig. 11:** Comparison of sedimentation rates (stars) at core location S2 with storm frequency (open
828 circles), defined as the number of water levels, exceeding 2.4 m (NN).

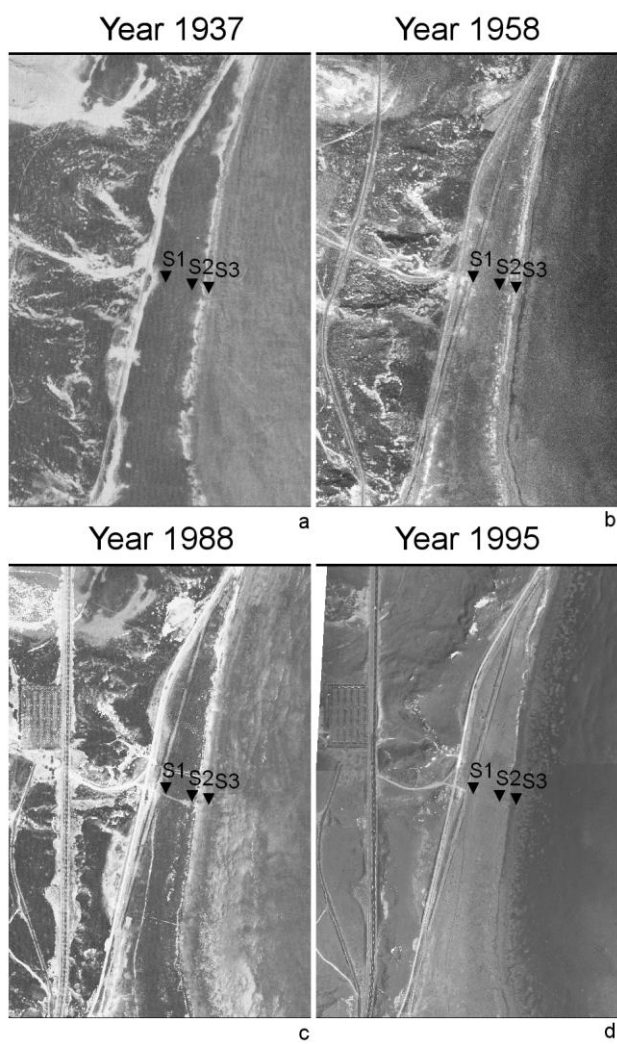
829 **Fig. 12:** Results of linear regression analysis: β - and p-values (circles and triangles respectively)
830 for different storm water levels (m above NN) are shown. β - and p-values refer to results of
831 multiple linear regression analyses of storm frequency (filled symbols) and storm intensity (open
832 symbols) with sedimentation rates at core location S2.

833 **Fig. 13:** Conceptual scheme of how vegetation is influencing accretion rates at various storm water
834 levels. The “No vegetation scenario” does not reflect the resuspension happening in absence of a
835 vegetation canopy.

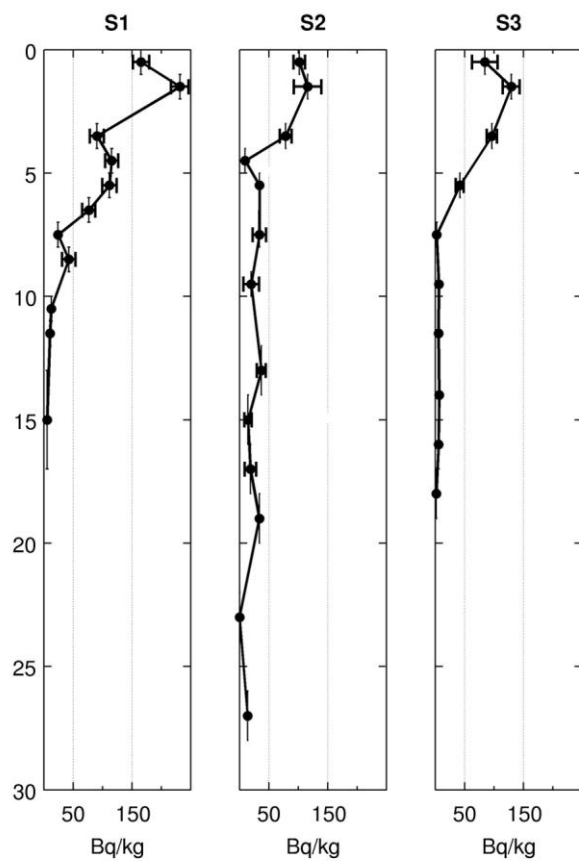




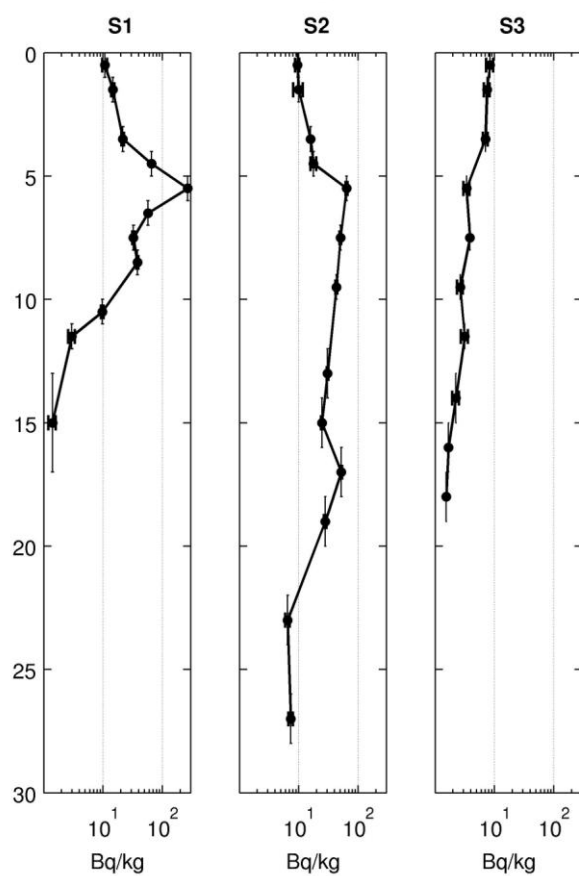
839



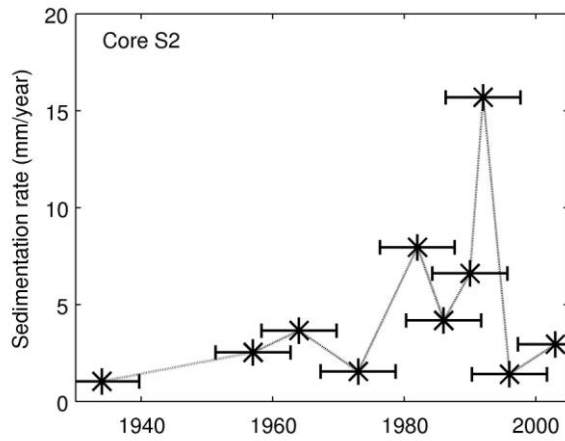
840



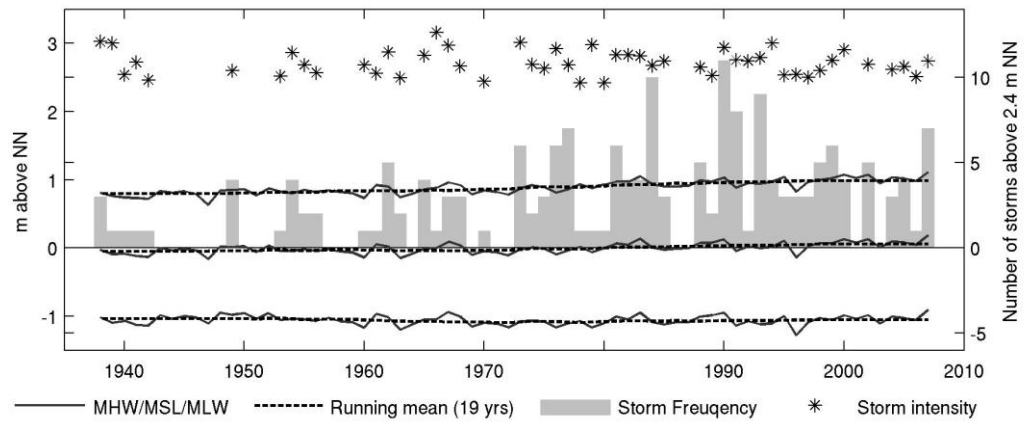
841



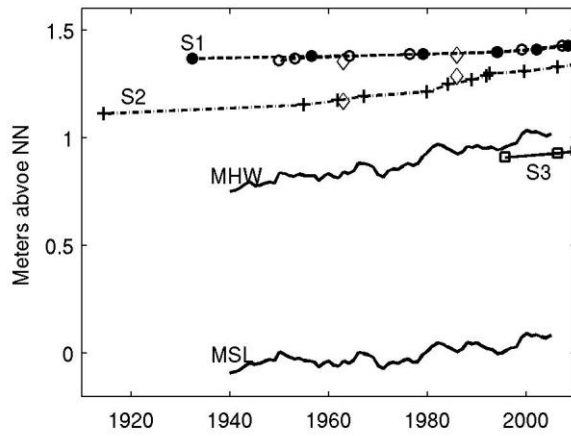
842



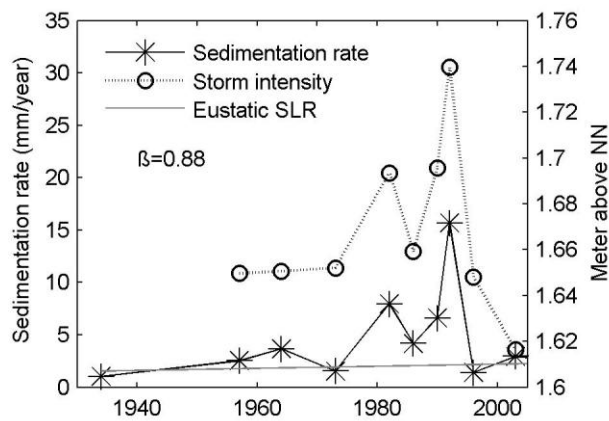
843



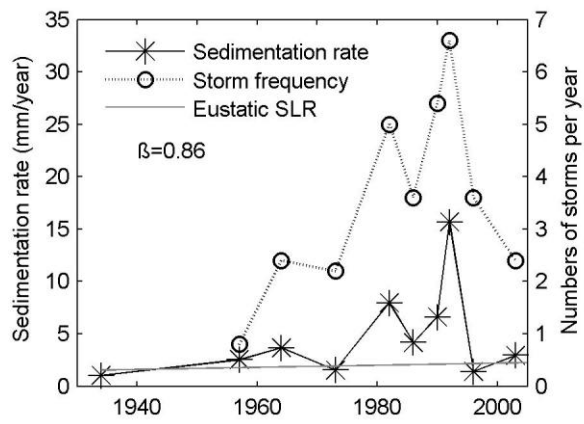
844



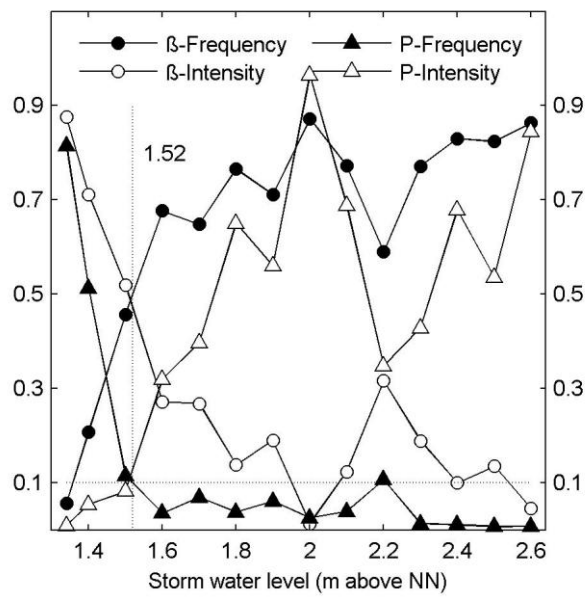
845



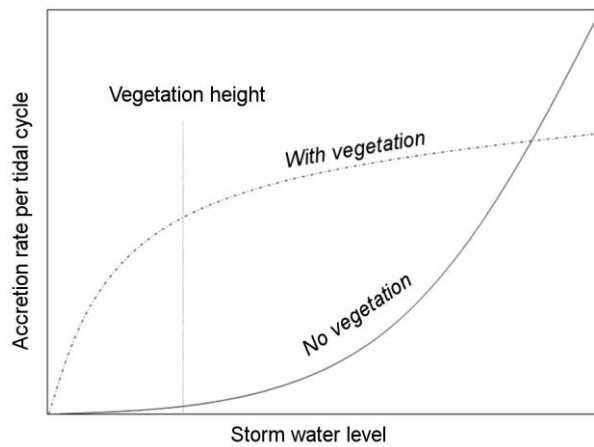
846



847



848



849

Figure 1
[Click here to download high resolution image](#)

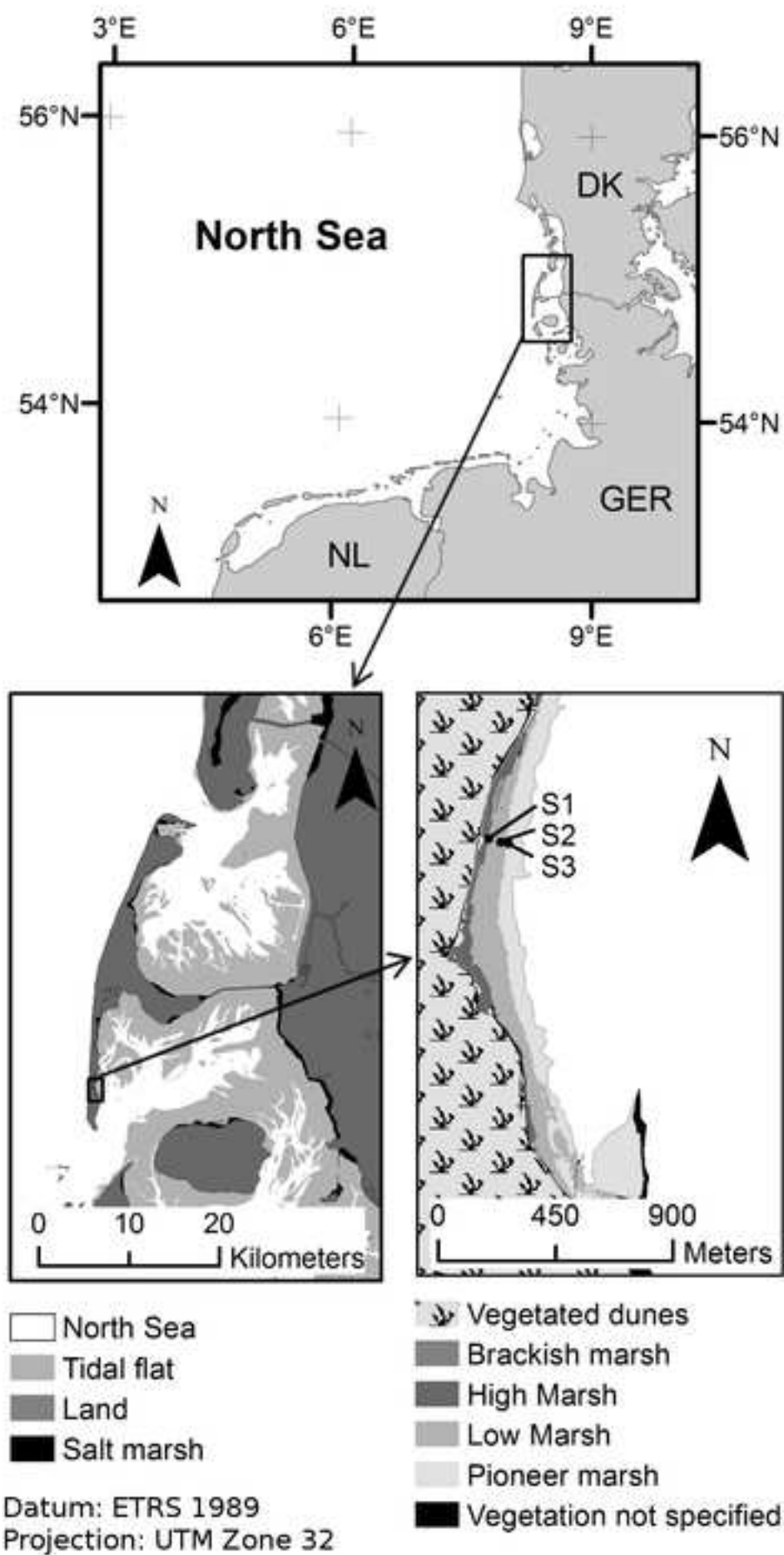


Figure 2
[Click here to download high resolution image](#)

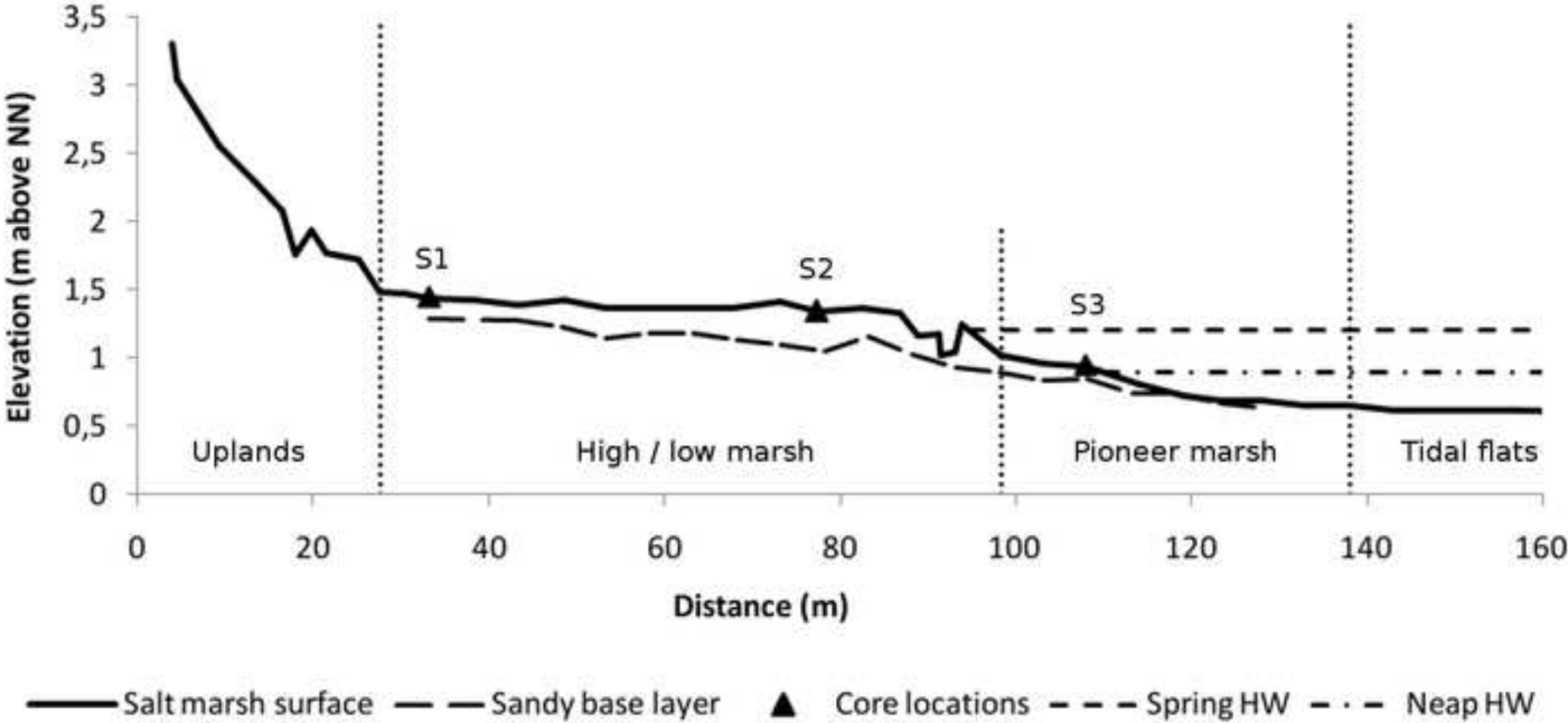


Figure 3
[Click here to download high resolution image](#)

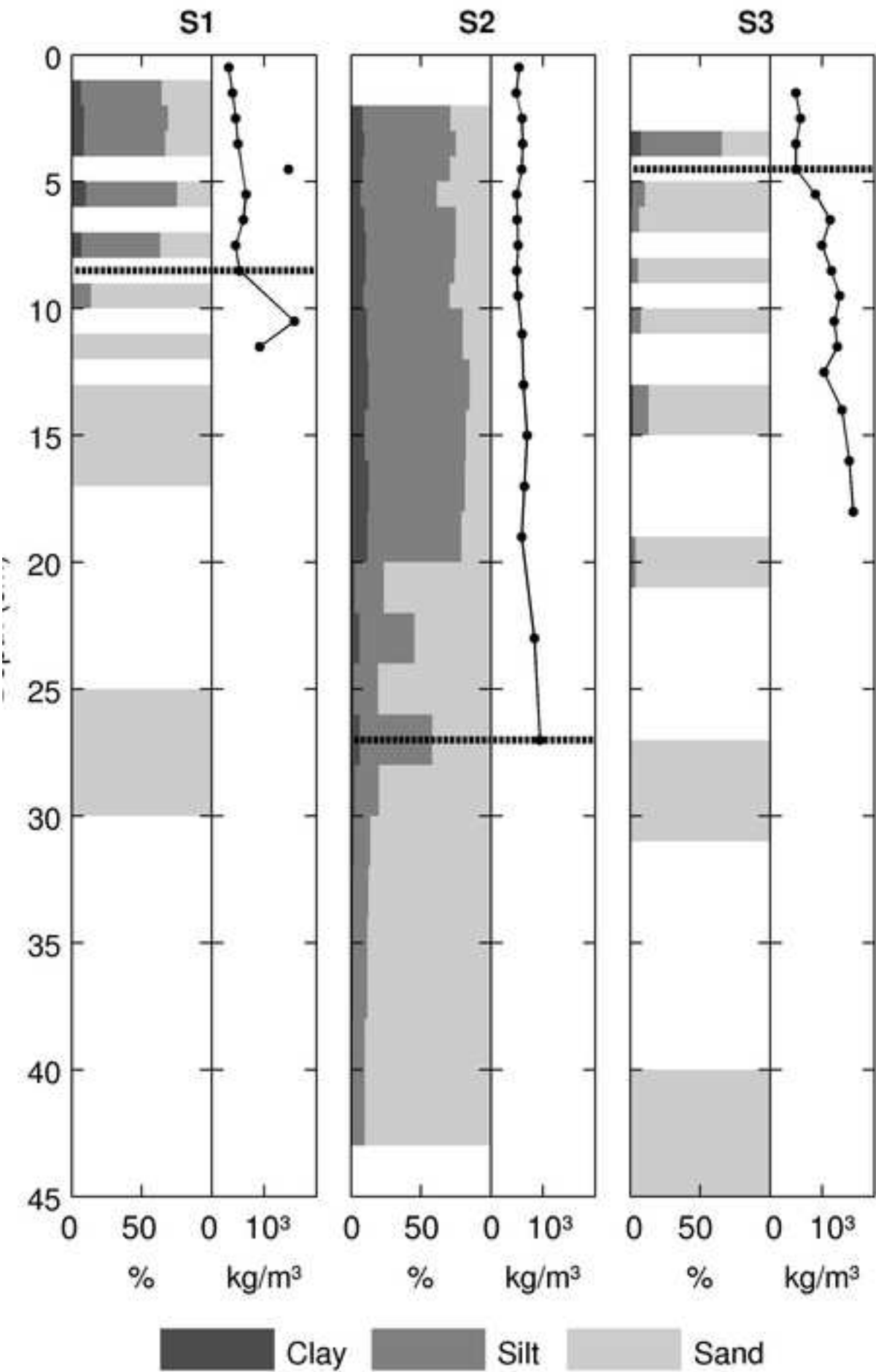


Figure 4
[Click here to download high resolution image](#)

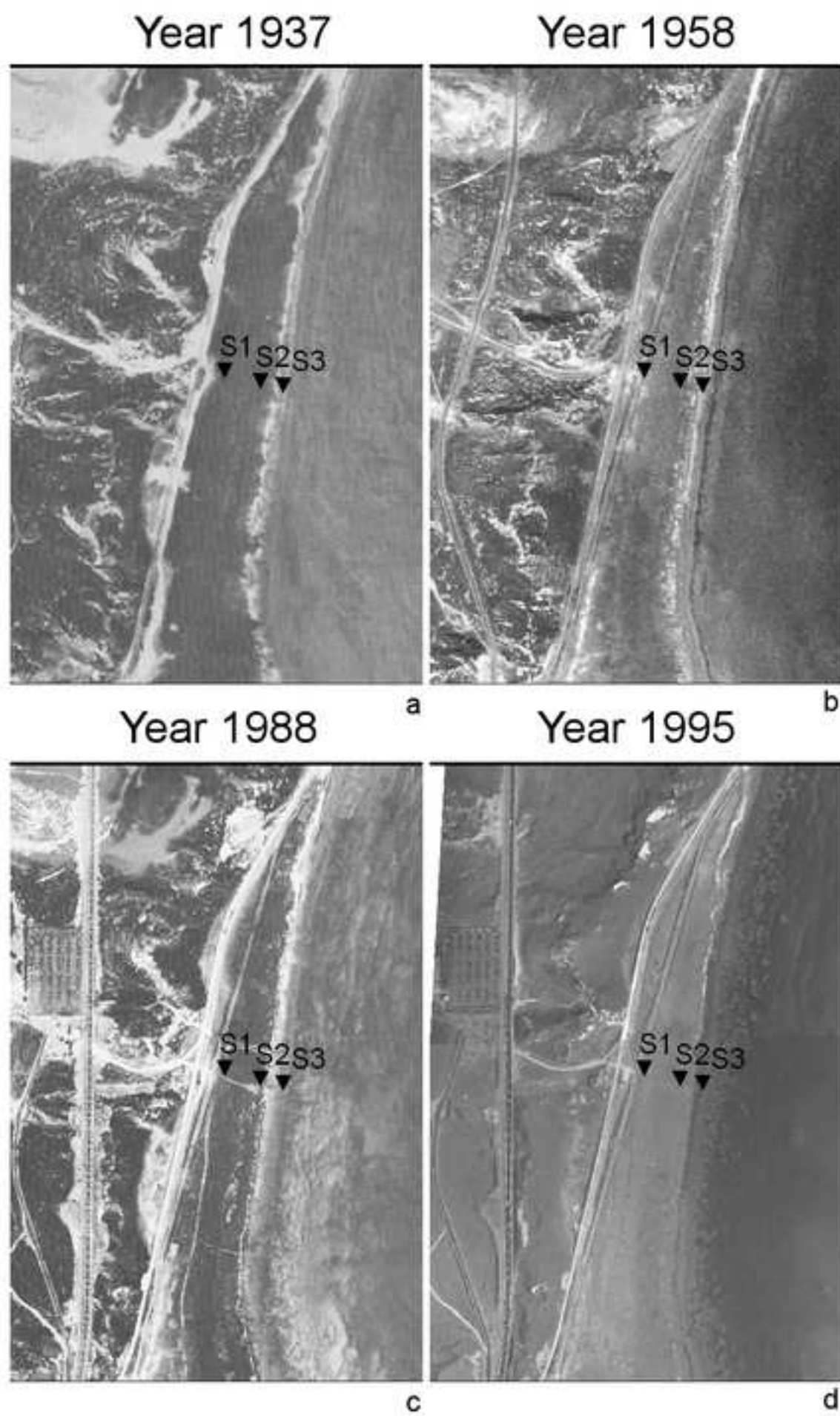


Figure 5
[Click here to download high resolution image](#)

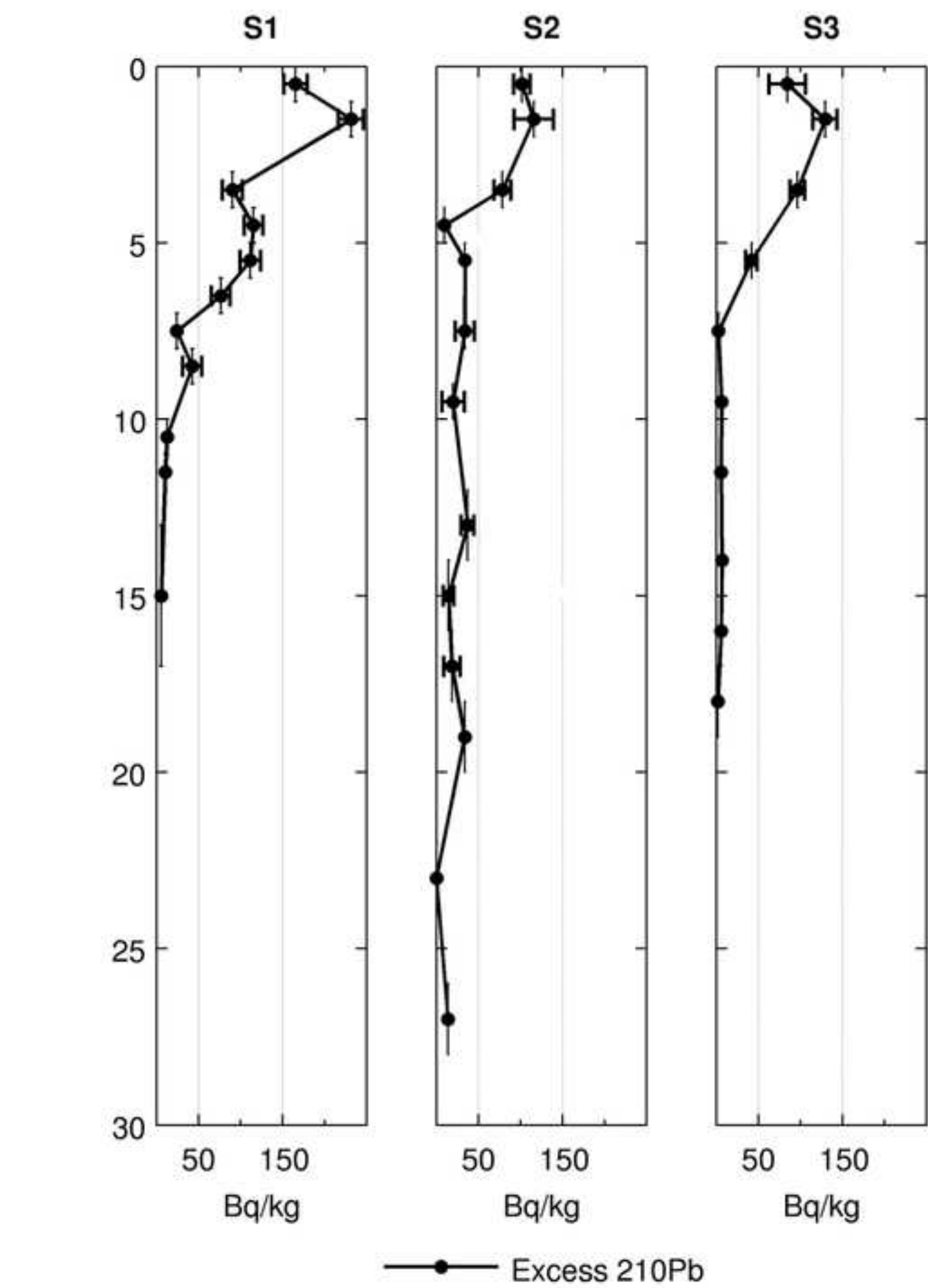


Figure 6
[Click here to download high resolution image](#)

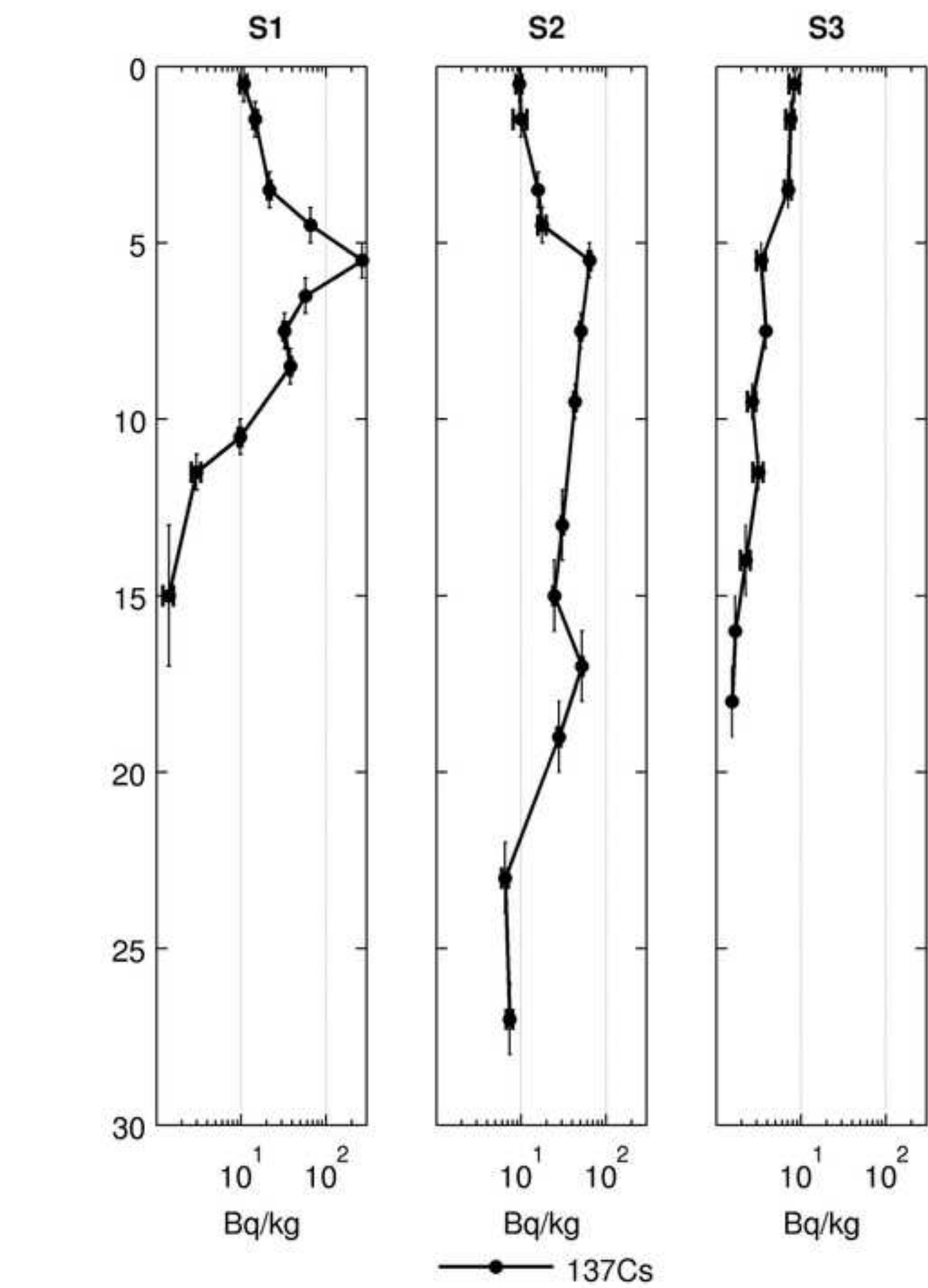


Figure 7
[Click here to download high resolution image](#)

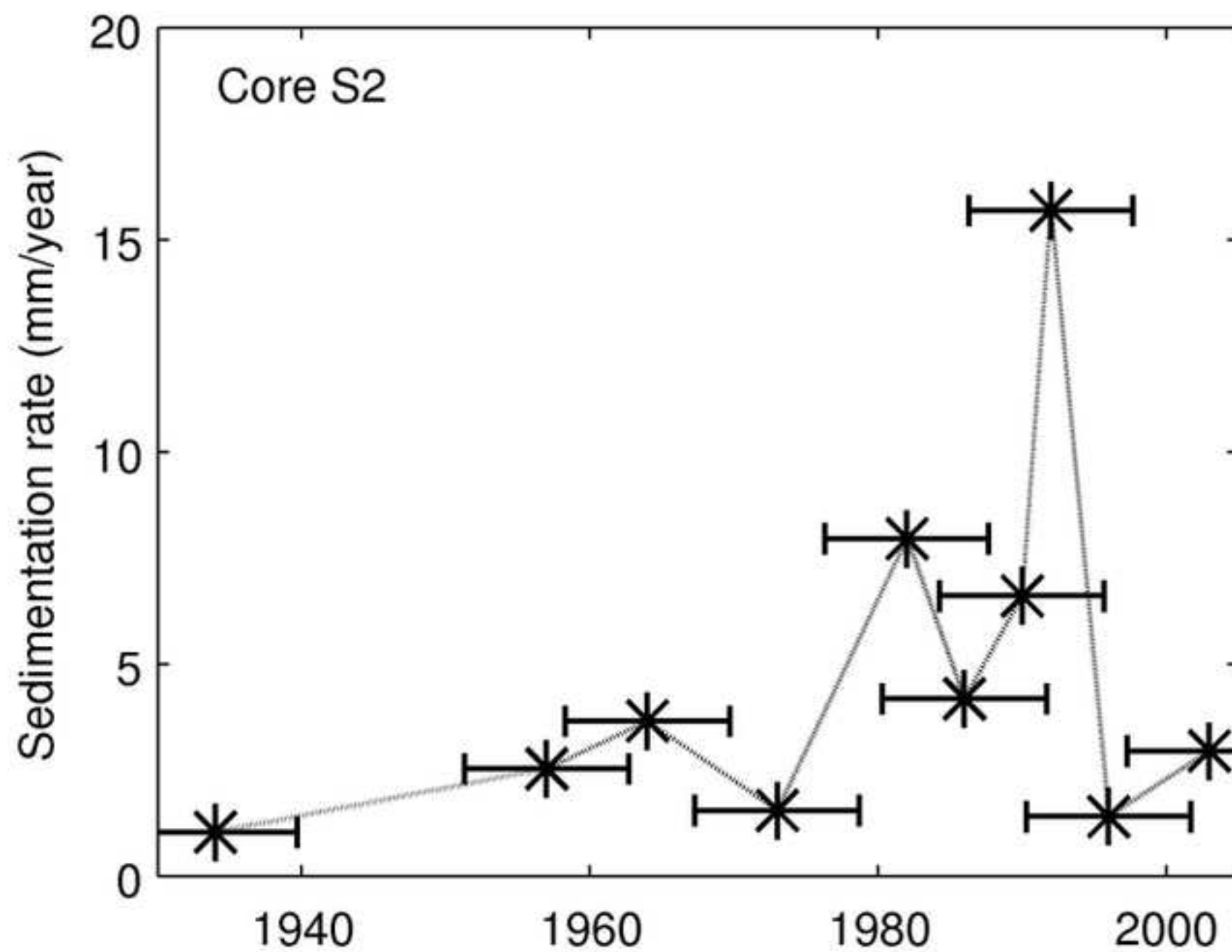


Figure 8
[Click here to download high resolution image](#)

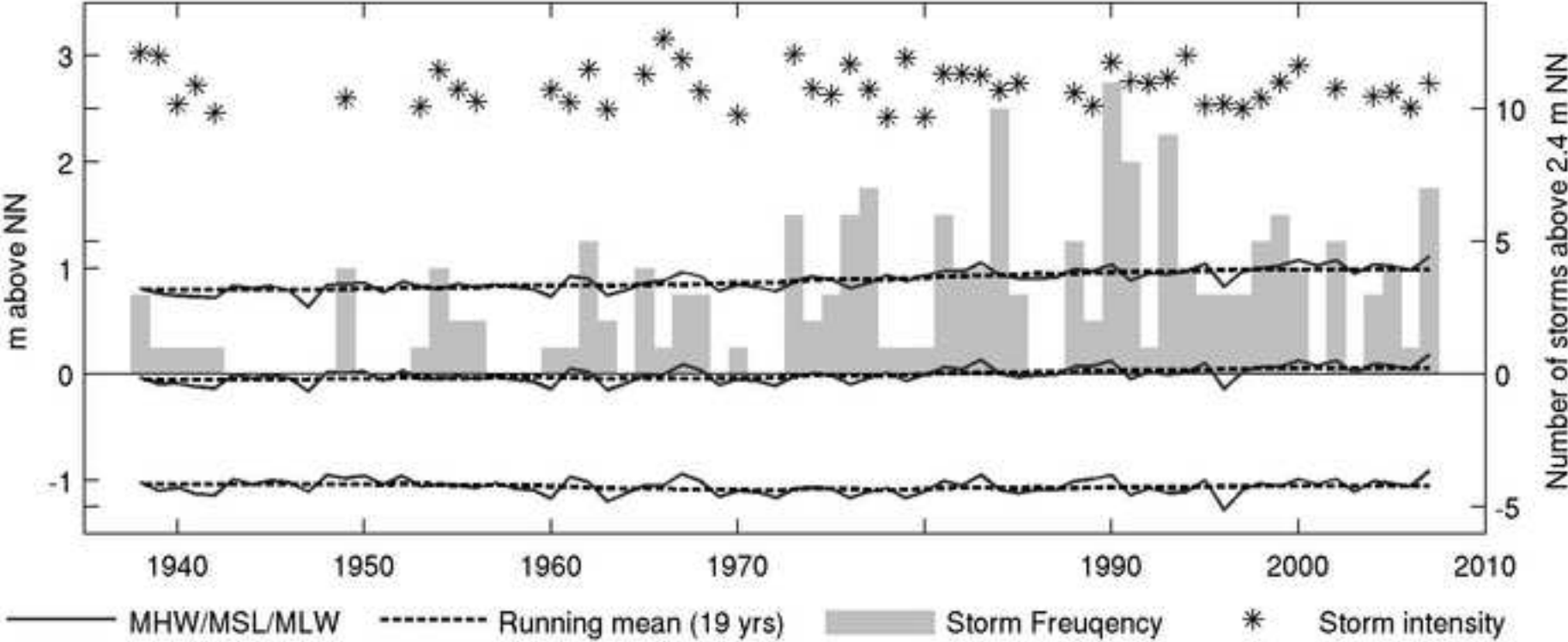


Figure 9
[Click here to download high resolution image](#)

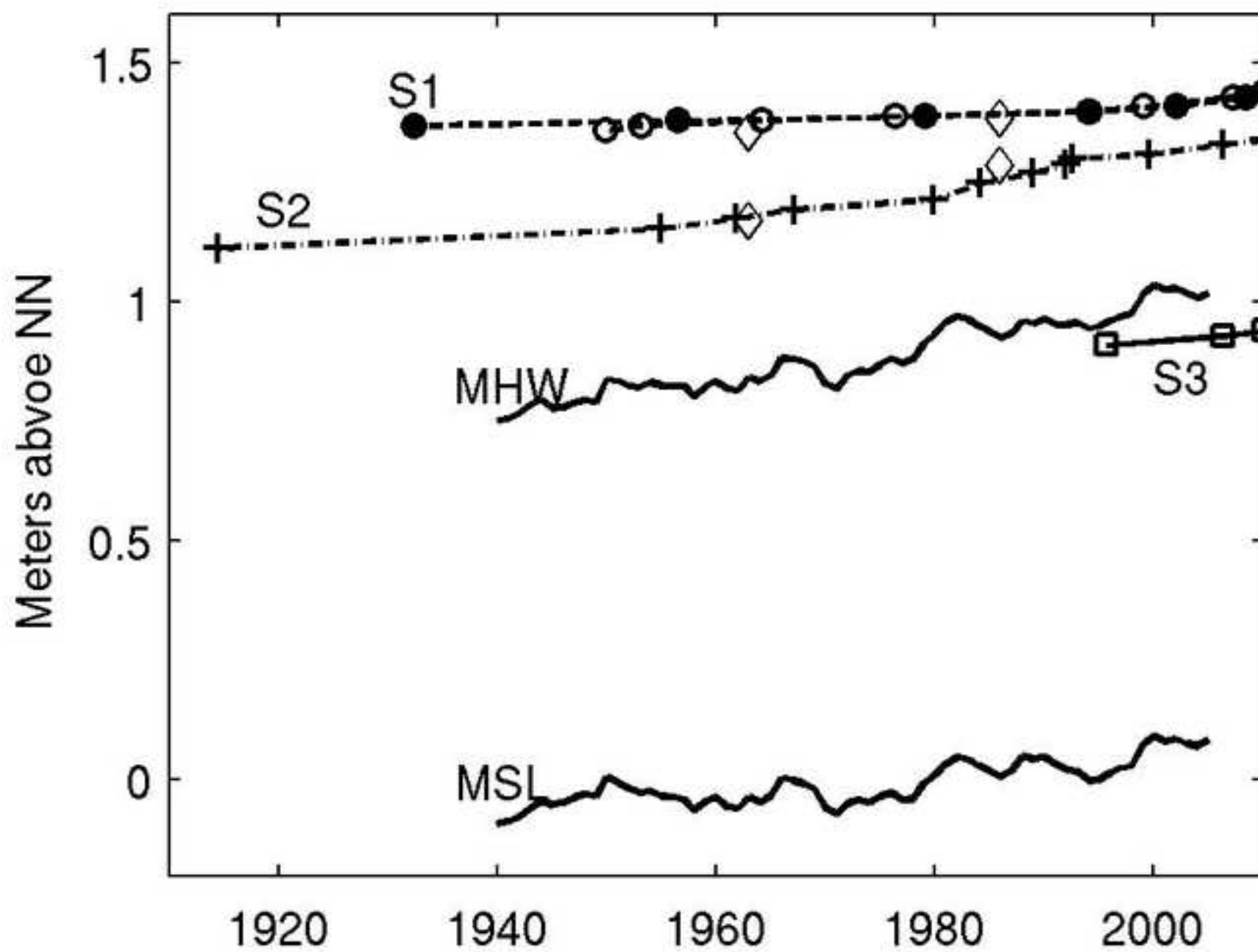


Figure 10
[Click here to download high resolution image](#)

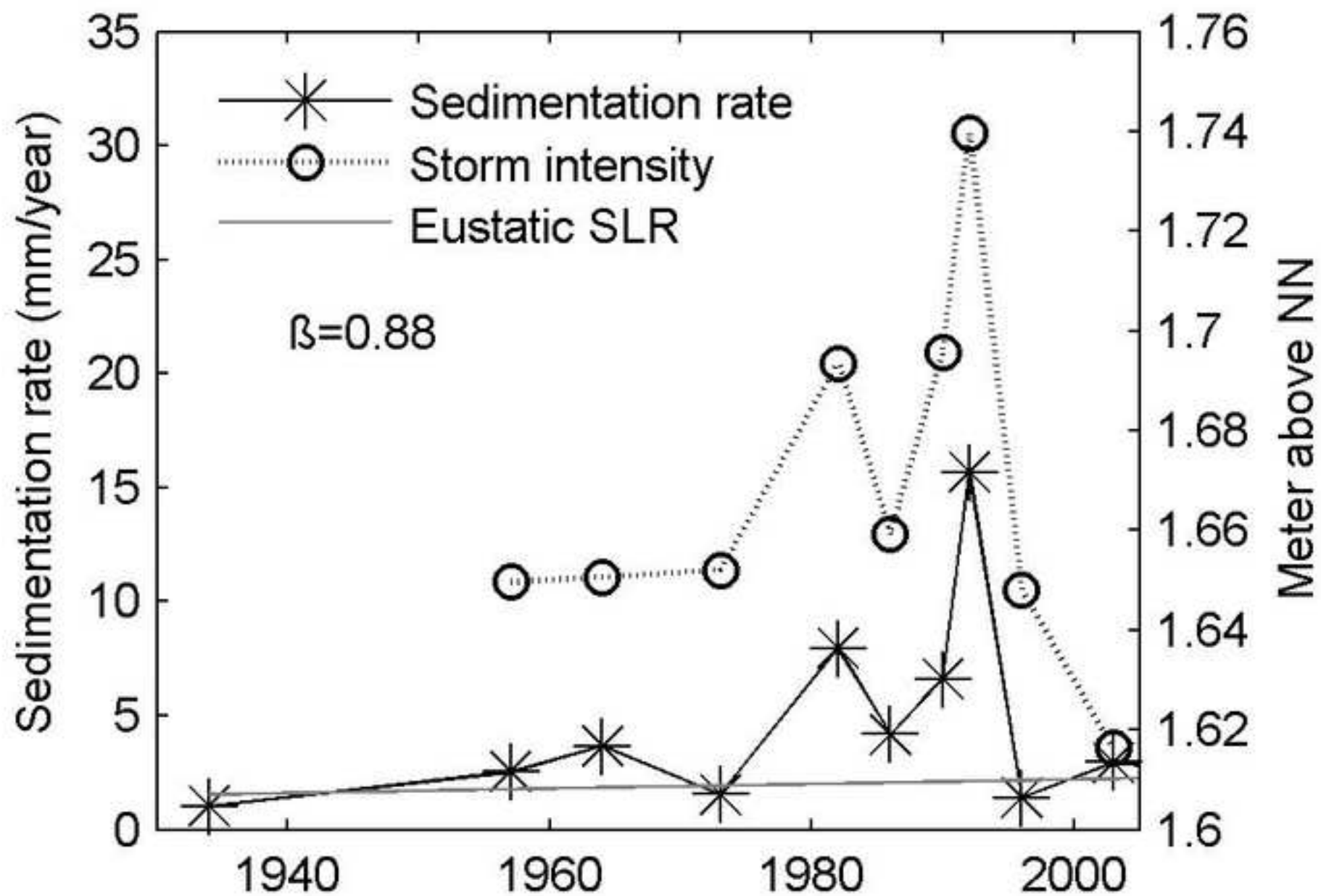


Figure 11
[Click here to download high resolution image](#)

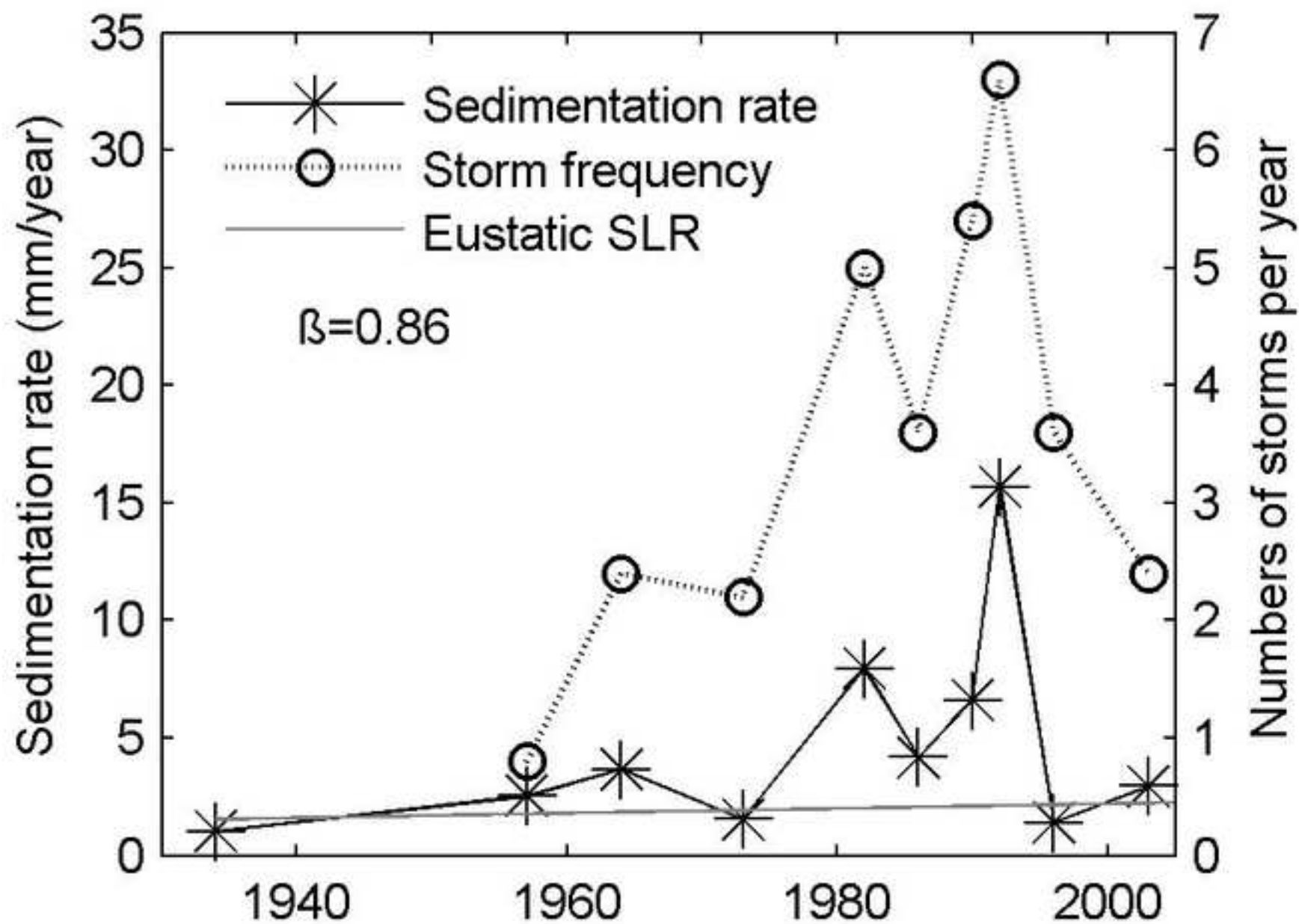


Figure 12
[Click here to download high resolution image](#)

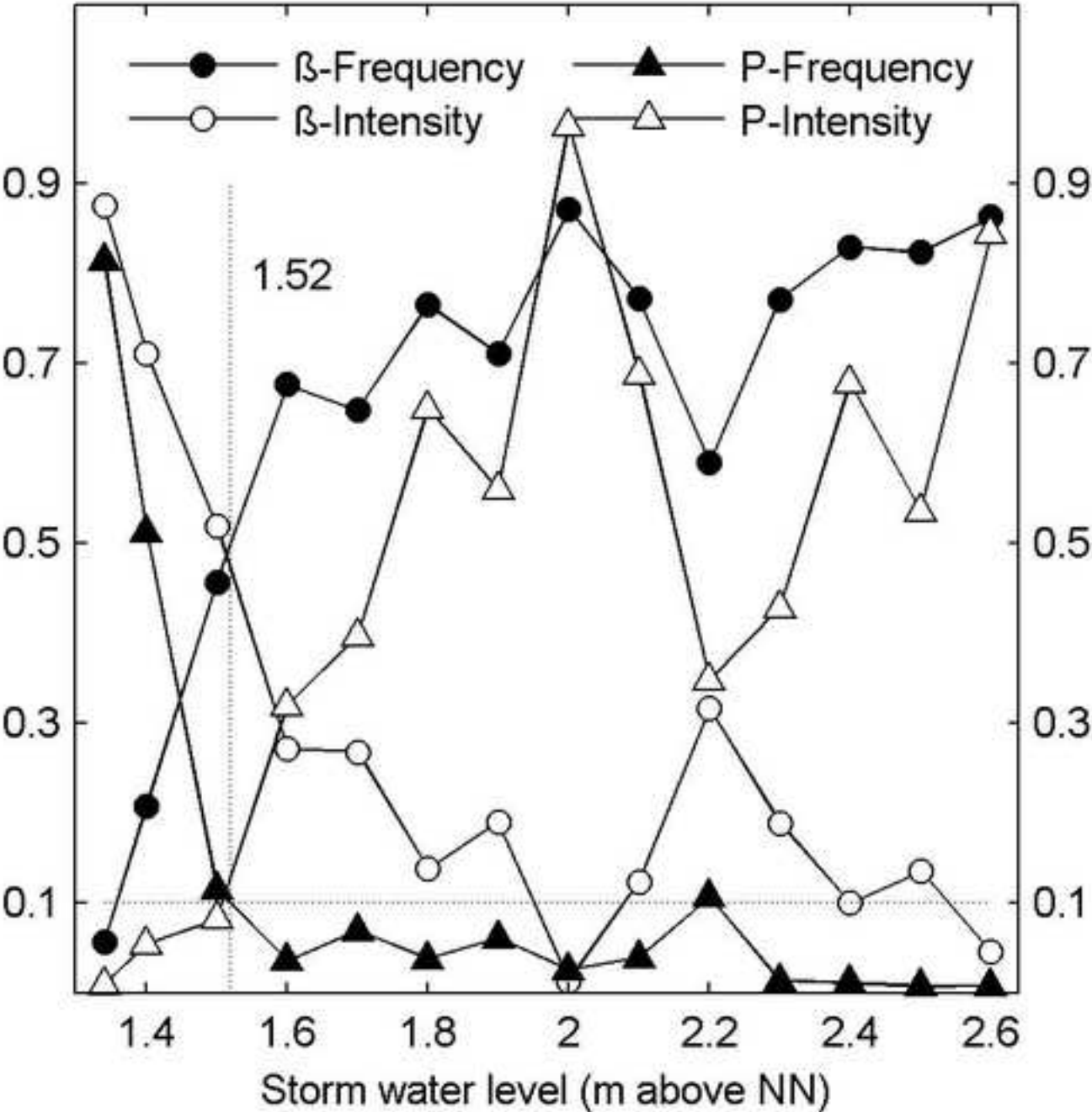


Figure 13
[Click here to download high resolution image](#)

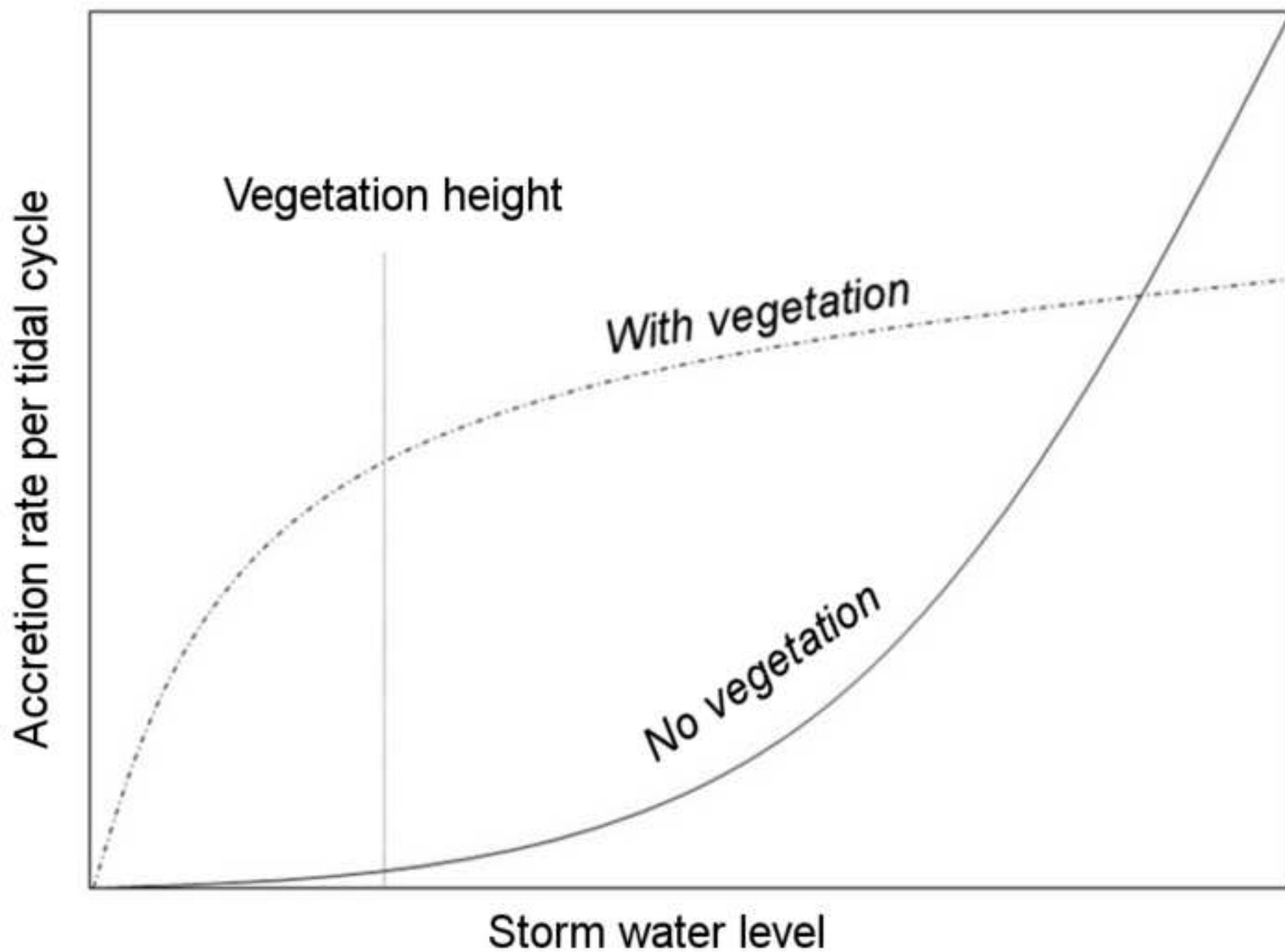


Table 1: Ages of base layers and mean sedimentation rates: Comparison of ²¹⁰Pb datings with information from aerial photographs.

Core name	Depth of base layer	Age of base layer (²¹⁰ Pb)	Age of base layer (aerial photographs)	Sedimentation rate (mm/year)
S1	8.5cm	1925-1955	<1937	1-1.2
S2	>27	1915	<1937	2.8
S3	4.5cm	1978-1988	1988-1995	2.5 (since 1996)